NATIONAL AERONAUTICS AND SPACE ADMINISTRATION

Technical Report 32-1325

A Lightweight 6½-ft Aeroshell for an Early Mars Probe Mission

R. G. Nagler and R. A. Boundy
Jet Propulsion Laboratory

J. R. Scholl and J. B. Dawson
Rohr Corporation

GPO PRICE $ ________

CSFTI PRICE(S) $ ________

Hard copy (HC) 3.00

Microfiche (MF) .65

ff 653 July 65

OCT 1968
RECEIVED
NASA STI FACILITY
INPUT BRANCH

FACILITY FORM 602

N68-35231 (ACCESSION NUMBER)	(THRU)
54 (PAGES)	1 (CODE)
CR-96994 (NASA CR OR TMX OR AD NUMBER)	31 (CATEGORY)

JET PROPULSION LABORATORY
CALIFORNIA INSTITUTE OF TECHNOLOGY
PASADENA, CALIFORNIA

September 15, 1968

NATIONAL AERONAUTICS AND SPACE ADMINISTRATION

Technical Report 32-1325

A Lightweight 6½-ft Aeroshell for an Early Mars Probe Mission

R. G. Nagler and R. A. Boundy
Jet Propulsion Laboratory

J. R. Scholl and J. B. Dawson
Rohr Corporation

Approved by:

Howard E Martens

Howard E. Martens, Manager
Materials Section

JET PROPULSION LABORATORY
CALIFORNIA INSTITUTE OF TECHNOLOGY
PASADENA, CALIFORNIA

September 15, 1968

TECHNICAL REPORT 32-1325

Copyright © 1968
Jet Propulsion Laboratory
California Institute of Technology

Prepared Under Contract No. NAS 7-100
National Aeronautics & Space Administration

Foreword

The design and engineering of the 6½-ft aeroshell described in this report was carried out at the Jet Propulsion Laboratory as part of the Capsule System Advanced Development (CSAD) Program. The aeroshell structure was fabricated under contract to JPL at the Riverside, California, facilities of Rohr Corporation. The ablator was formulated and applied to the structure at the Space Systems Division of Avco Corporation, Lowell, Massachusetts.

Contents (contd)

Appendix. Specification for Aeroshell Fabrication 42

References 45

Tables

1. Configuration variations in advanced development program 2
2. Materials used on $6\frac{1}{2}$-ft-diam aeroshell 5
3. Variation in ablator thickness along cone 37

Figures

1. Small developmental aeroshells 3
2. Adhesive comparison 4
3. Flexure strength of honeycomb-sandwich composites with different facesheet resin systems 4
4. Core cell shape comparison 5
5. Alternate core splicing techniques 6
6. Schematic of aeroshell design for Mars probe 7
7. Beryllium nose dome detail 8
8. Schematic of major tool assembly 12
9. Major bond jigs 12
10. Closeup of detail parts 13
11. Stretchforming setup 14
12. Schematic of titanium part clamping arrangement 15
13. Aft cone assembly after first cure and with the core machined 15
14. V-ring splice 16
15. V-ring and potting compound in place 17
16. Texture of 4-ply phenolic-fiberglass facesheet on aft stiffening cone 17
17. Completed aft stiffening cone 18
18. Laying up first facesheet on major cone 18
19. Outer facesheet on major cone, freestanding 18
20. Forming honeycomb core for major cone 19
21. Splicing honeycomb core for major cone 19

PRECEDING PAGE BLANK NOT FILMED.

Contents

I. Introduction 1

A. Principal Problems 1

B. Early Material and Fabrication Development 1

II. Design and Prefabrication Work 5

A. Detail Design 5

B. Tooling 11

III. Detail Fabrication of Basic Cone 13

A. Detail Parts 13

B. Aft Cone Assembly 15

C. Major Cone Assembly 15

D. Mating the Major and Aft Cones 21

E. Finishing and Mating the Attachment Ring 23

F. Routing and Drilling the Forward Ring 24

IV. Inspection of Basic Conical Structure 25

V. Nosecap and Ablator 30

A. Steel Dome 30

B. Ablator Application and Machining 30

VI. Final Inspection of Completed Aeroshell 30

VII. Repair Techniques 34

VIII. Supplementary Studies and Tests 38

A. Sterilization 38

B. Vacuum 38

C. Honeycomb-Sandwich Thermal Gradient 39

D. Insert Retention 39

E. Core Splice Effects 40

F. Titanium Joining 40

G. Metal Dome–Ablator Joint 40

IX. Summary 41

Contents (contd)

Figures (contd)

22. Major cone with core cured in place 19

23. Machined surface at forward ring 20

24. Potting lightweight epoxy foam at V-ring locations 20

25. Laying up second facesheet on major cone 20

26. Vacuum-bag setup 21

27. Cross section of vacuum-bag layup 22

28. Sealing joint between two bond jigs for vacuum-bagging 22

29. Texture of inner skin on major cone 23

30. Completed major cone 23

31. Placing feeler gages between two cones to determine adhesive requirements at joint 23

32. Potting compound being gunned into mating groove 23

33. Fitting C-rings in place 24

34. Inserts in place in attachment rings 24

35. Attachment ring with potting compound being troweled in place over inserts 24

36. Applying adhesive over potted attachment ring 25

37. Aeroshell entering oven for final cure 25

38. Drilling holes at forward ring 25

39. Front view of finished structure 26

40. Rear view of finished structure 26

41. Inspecting core-to-facesheet bond 27

42. Out-of-round inspection setup at Rohr 28

43. Polar chart of out-of-round measurements on structure 29

44. Spherical metallic dome 30

45. Dome in place on structure 30

46. Aeroshell structure mounted on coating fixture 31

47. Roller-coating ablator on major cone 32

48. The ablator vacuum-bagged 33

49. Aeroshell with cured ablator mounted on machining fixture 33

50. Machined ablator surface at dome interface 34

51. Machined conical ablator surface 34

Contents (contd)

Figures (contd)

52. The completed aeroshell 35

53. Aeroshell on inspection fixture at JPL 35

54. Heat shield *thickness-determination* setup 35

55. Dial indicator with pointed tip 36

56. Final inspection of aeroshell 36

57. Facesheet repair technique 36

58. Core repair area 37

59. Comparison of before and after sterilization samples 38

60. Laminate flexure test setup in a vacuum 39

61. Flatwise tension test setup in a vacuum 39

62. Schematic of flatwise tension test with one hot face 40

63. Test setup for insert pull strengths 40

64. Loop retainers for critical ablator joint 41

Abstract

Mars provides new challenges in the design of survivable atmospheric probes. This report analyzes the problems of and presents a design concept for meeting those challenges. A lightweight, 6½-ft-diam, sphere-cone, honeycomb-sandwich structure with an elastomeric ablator is described which is almost an order-of-magnitude lighter per unit area than those in the manned space program, allowing atmospheric deceleration at densities equivalent to very high altitudes on earth. This structure is made primarily from phenolic fiberglass for ease of fabrication and RF transparency, but titanium rings are used as stiffeners at the outer edge. Details of the fabrication are delineated, and the results of supplementary studies to prove structural reliability and environmental compatibility are given. This type of structure is easily fabricated under normal shop practices; and experience with constructing two of the 6½-ft-diam aeroshells indicates that lightweight, 20-ft-diam (or larger) aeroshells can be fabricated to reasonably close tolerances.

A Lightweight 6½-ft Aeroshell for an Early Mars Probe Mission

I. Introduction

A. Principal Problems

The idea of entering into the atmosphere of Mars and landing on the planet tantalizes the mind. To perform such a quest, new developments in lightweight structures are needed to maximize the science payload delivered to the planet without compromising mission reliability. The Mars atmosphere is very tenuous. Typical surface pressures at Mars are of the order of the earth pressures at an altitude of 200,000 ft. Aerodynamic deceleration in this low density atmosphere to impact survivable velocities presupposes a very low vehicle weight per unit area. Ballistic coefficients in the range of 0.1 to 0.2 slugs/ft^2 are typical. This is about an order of magnitude lighter per unit area than the vehicles in our more extensive manned space program.

To match the low magnitude of the entry deceleration loads to the lightest-weight structure possible, consideration of the minimum gage in each of the potential shell-construction alternates becomes important. Cost limitations, on the other hand, necessitate maximizing use of state-of-the-art technology. Preliminary structural configuration studies at JPL have shown that, except for certain exotic composite-material configurations, which for the most part are not available, honeycomb sandwich appears to show the widest applicability to a variety of potential missions. Monocoques and other common alternates appear to be comparatively heavy, and in some cases, less adaptable to such specific mission requirements as atmospheric sampling and RF transparency. The development of a lightweight honeycomb-sandwich structure for an early Mars entry probe mission is outlined here. Two 6½-ft-diam aeroshells were made as demonstration models.

B. Early Material and Fabrication Development

At an early stage in selecting structural configurations for a variety of hypothetical missions, it became obvious that lack of design data made choice of a specific configuration as hypothetical as the mission itself. Comparison of similar, but heavier, structural alternates indicated that maximum rigidity and strength could be obtained from honeycomb-sandwich structures, providing the projected decreases in weight could be fabricated without reduction in the anticipated strengths.

An extensive development effort was undertaken to define minimum-gage fabrication in both metallic and reinforced-plastic honeycomb sandwich, to optimize the material systems, to establish reproducible methods of manufacture in both flat and doubly curved samples, and to provide design data useful in analyzing structural configurations for the large variety of missions under study (Ref. 1). An outline of the configuration variations considered is provided in Table 1. All of these material configurations were fabricated in flat samples and were tested in flatwise tension, flatwise compression, plate shear, sandwich flexure, edgewise compression, and sandwich peel – both parallel and perpendicular to the core ribbon direction, where pertinent. The material combinations showing the most promise were further tested (1) for high (+350°F) and low (−150°F) temperature properties, (2) for flatwise tension strength with one facesheet at 600°F for a short time, (3) for compatibility with ethylene oxide and dry-heat sterilization, (4) and for vacuum stability and strength effects. Some of these combinations were also fabricated into the small, doubly curved aeroshell models shown in Fig. 1.

Some of the important conclusions in fabricability from this early, advanced development program include:

1. *Resin fiberglass* honeycomb-sandwich configurations tend to be lighter in weight, easier to fabricate, and more reproducibly reliable than do similar configurations of minimum gage in high-strength aluminum honeycomb sandwich construction.
2. For this lightweight construction, the thinnest gage, unsupported film adhesive available gives as good or better a bond between the facesheet and core than does (1) thicker, unsupported film, (2) any supported films, or (3) paste adhesive. (Compare filleting in Fig. 2.)
3. For similar resin contents, facesheet strength is scalable to cloth thickness with little variation in specific strength down to cloth sizes of about 4 mils (style 112). Fabricability does not change particularly, except that the plain weave of the styles 112 and 116 cloth and the 8-harness satin weave of the style 181 cloth were much easier to form around sharp radii than the crowfoot satin weave of style 120 cloth.
4. At room temperature and in these sandwich configurations, the facesheet resin contributes only slightly to differences in the overall composite flexure strength, providing other parameters (adhesive, core, etc.) in the configuration are not changed, and providing the particular resin used is one of the best high-temperature resins of its generic class (see Fig. 3). Observed variations are as often attributable to such minor inconsistencies as the differences in technician attitude at the time of fabrication. Resin selection is thus more dependent

Table 1. Configuration variations in advanced development program

Structural item	Configuration Variations	
	Fiberglass sandwich	Metallic sandwich
Facesheet	Resin: phenolic, epoxy, epoxy novalac, polyester, polyimide Glass type: E glass, S glass Glass weave: style 108, 112, 116, 120, and 181 Glass finish: Volan A, A-1100, S-935 Number of plies: 2, 4, 6, 12 Rotation of plies: 45 and 60 deg Ply overlap: aligned, staggered Doubler discontinuities: aligned, staggered	Material: 2024-T4, 5056, 5052 Thickness: 5, 10, and 15 mils
Core	Resin: phenolic, polyimide, nomex Cell shape: hexagonal, flexcore, dovetail Cell size: 3/16 and 1/4 in. Cell density: 3.5, 4.0, and 4.5/ft^3 Thickness: 1/2, 3/4 in. Core splice: film, foam, and 1-in.-crush overlap	Material: 2024-T4, 5056, 5052 Cell shape: hexagonal Cell size: 3/8 and 1/4 in. Cell density: 3.4 and 4.2 lb/ft^3 Thickness: 1/2 in.
Adhesive	Resin: epoxy, epoxy phenolic, polyimide Thickness: 4 to 12 mils Supported and unsupported	Resin: epoxy Thickness: 4, 8, and 12 mils Supported and unsupported

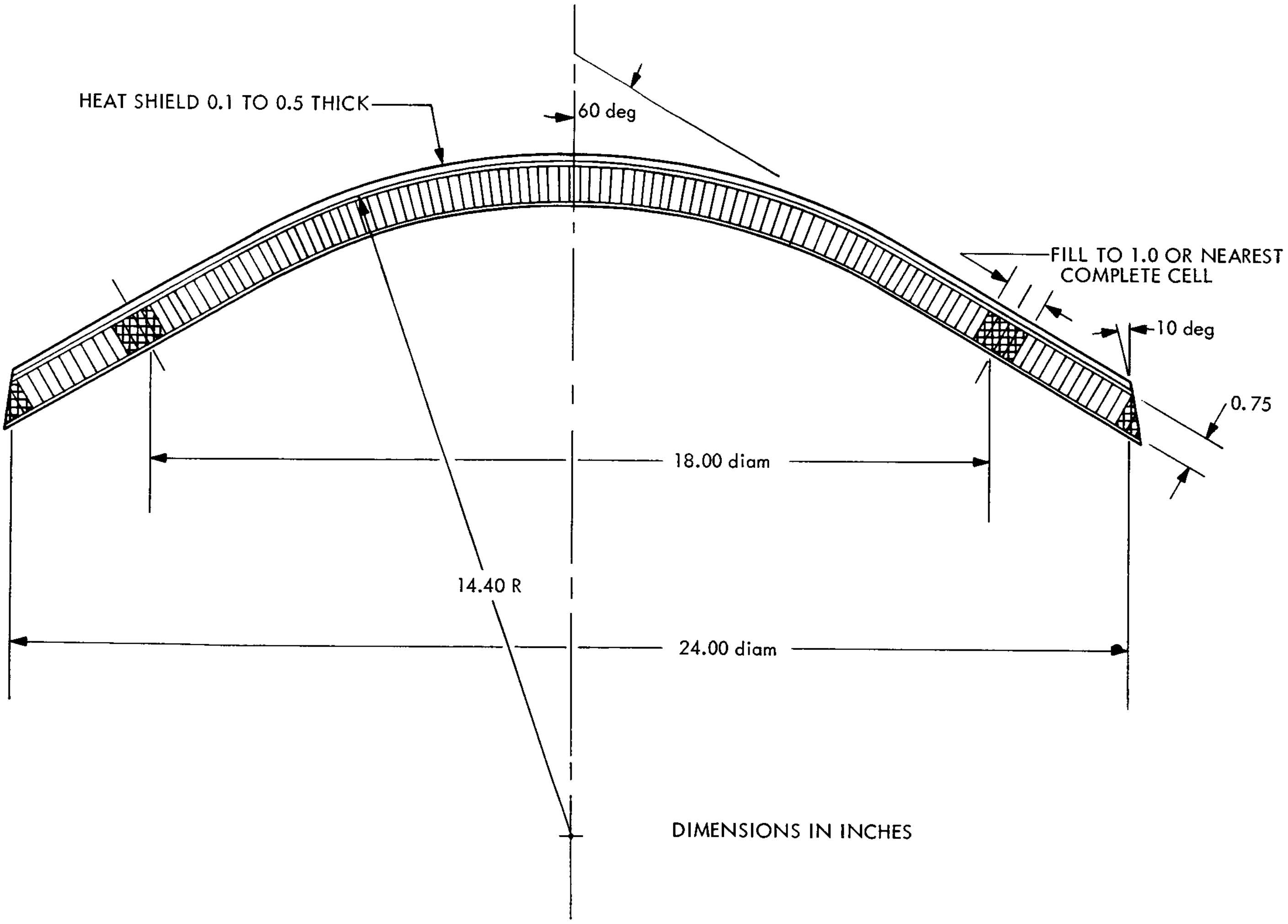
HEAT SHIELD 0.1 TO 0.5 THICK
60 deg
FILL TO 1.0 OR NEAREST COMPLETE CELL
10 deg
0.75
18.00 diam
14.40 R
24.00 diam
DIMENSIONS IN INCHES

Fig. 1. Small developmental aeroshells

(a) UNSUPPORTED 4-mil EPOXY FILM ADHESIVE

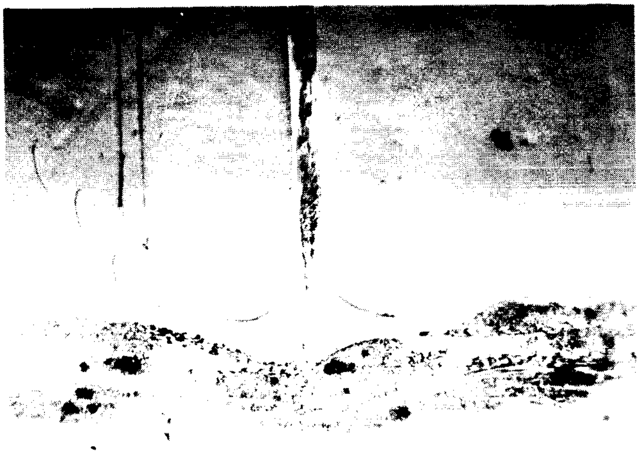

(b) NYLON-CLOTH-SUPPORTED 8-mil EPOXY FILM ADHESIVE

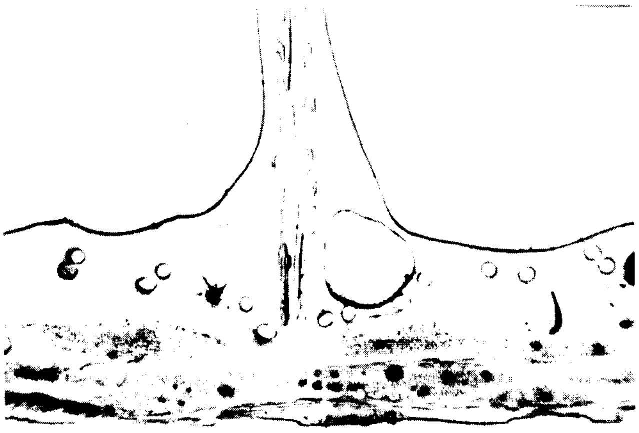

(c) ALUMINUM-FILLED EPOXY PASTE ADHESIVE

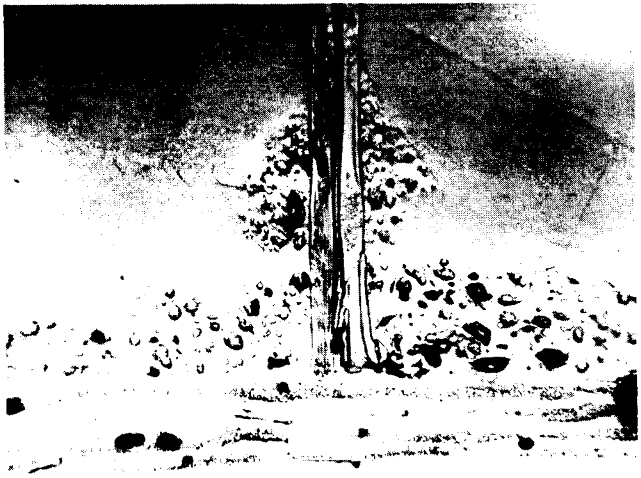

Fig. 2. Adhesive comparison

- ALL SAMPLE LENGTHS SUFFICIENT TO CAUSE FACING FAILURE
- SHADED REGIONS REPRESENT SCATTER IN FIVE REPLICATES
- ROOM TEMPERATURE ONLY

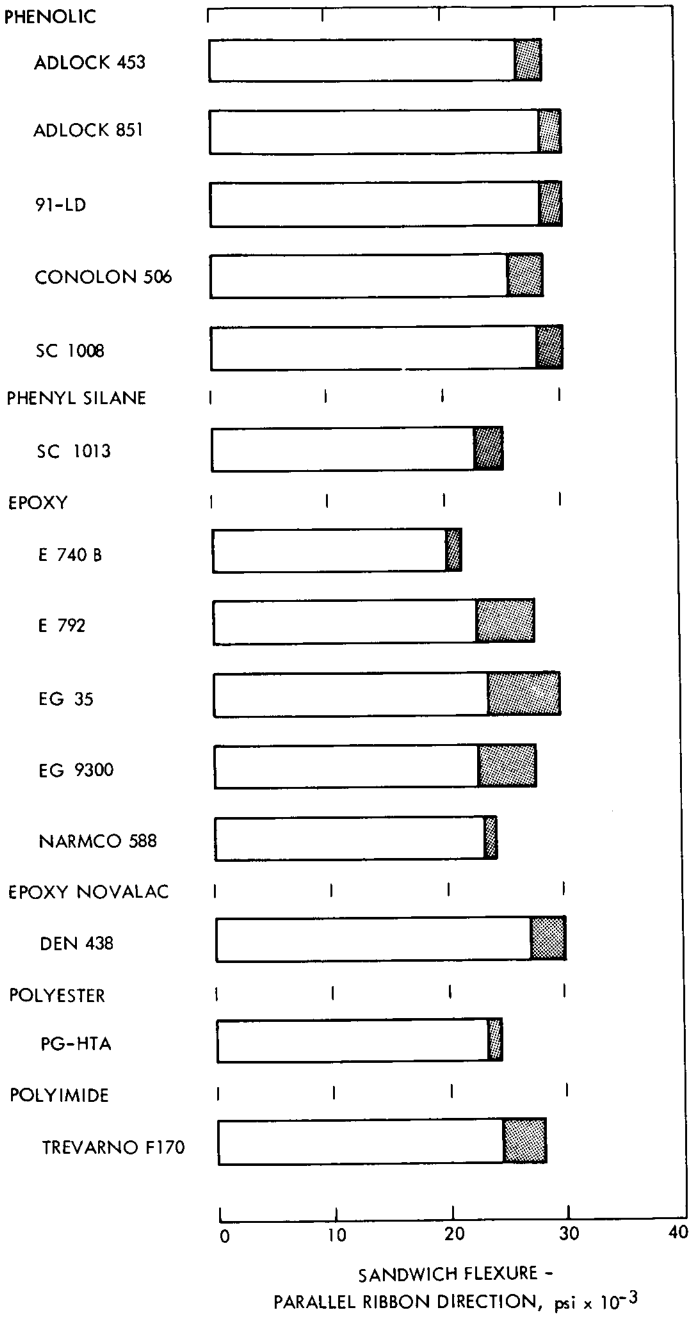

Fig. 3. Flexure strength of honeycomb-sandwich composites with different facesheet resin systems

on high- and low-temperature effects, sterilization, and vacuum compatibility. Phenolic and polyimide composites appear best from this view, with the phenolic slightly easier to fabricate reproducibly.

5. Four plies of preimpregnated fiberglass at 45-deg rotations appear to be a reasonably isotropic, minimum gage under relaxed fabrication procedures. Two and three plies are also feasible as reasonably isotropic structures if special care is taken in cloth selection and composite fabrication.

6. When molded in the partially cured condition, hexagonal-shaped core forms adequately to doubly curved surfaces at least as sharp as the aeroshell shown in Fig. 1 and provides stronger, less dense structures than the best available flexcore or dovetail core. The three, core cell shapes are shown in Fig. 4.

7. In the 3/16-in. cell size, one cell crush-overlap core splices are lighter than foam or film-adhesive-spliced core of equivalent splice strength (see alternates in Fig. 5).

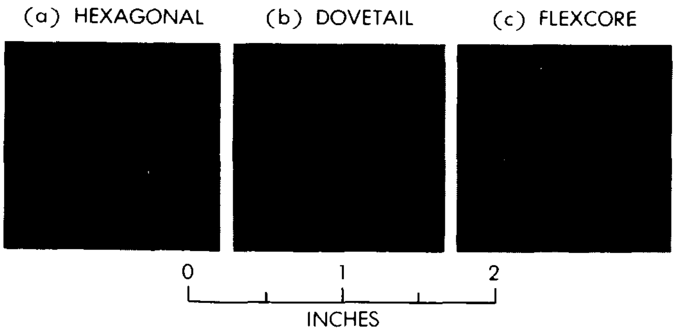

Fig. 4. Core cell shape comparison

II. Design and Prefabrication Work

A. Detail Design

The 6½-ft-diameter aeroshell shown in Figs. 6 and 7 was structurally designed by use of a computer program for unsymmetrically loaded thin shells of revolution (Ref. 2). In this program, the honeycomb sandwich is treated as a thin shell with an equivalent or effective modulus. The specific materials used in the fabrication are summarized in Table 2. These materials are not considered to be optimum, but they were chosen at an early stage in the development program discussed earlier. Their mechanical and physical properties are adequate to meet both the design requirements and the anticipated environmental tests discussed later in this report.

Table 2. Materials used on 6½-ft-diam aeroshell

Structural item	Material
1. Facesheets and reinforcement rings	American Reinforced Plastic's Adlock 851 phenolic resin impregnated on E glass cloth with a Volan A finish; resin content 45, ±3%
Individual facesheets	Six plies of style 112 cloth (4 mils each); locally, 4 to 12 plies of style 112 cloth.
Three edge-reinforcement rings	Style 112 cloth, 7 plies
Attachment ring skin	Style 112 cloth, 2 outer plies, and style 181 cloth, 5 inner plies (50 mils total nested)
Forward reinforcement laminate	Style 181 cloth, 15 plies
2. Aft cone facesheet and U-ring	Commercially pure titanium, Mil-T-9046 Class 7, 15-mil facesheet, 20-mil U-ring
3. Core	Honeycomb Products, Inc. HTP hexagonal core, 3/16-in. cell, 3/4 in. thick, 4.0 lb/ft^3 density, phenolic impregnated style 112 E glass
4. Foam potting compound	Rohr Corp. M323 V high-temperature epoxy foam, 31.2 lb/ft^3 density
5. Film adhesive	Bloomingdale Rubber Co. FM96U unsupported epoxy film, 0.03 lb/ft^2, and FM96 supported epoxy film on style 112 E glass cloth
6. Foam adhesive	Bloomingdale Rubber Co. FM40 epoxy foam adhesive film
7. Inserts	Shur-Lok Corp. SL601-3-4C
8. Fore expansion gasket	Teflon (TFE)
9. Fore joint insulators	Sintered silica foam of 25 lb/ft^3 density on flight model, phenolic fiberglass stock laminate on demonstration model
10. Heat shield	Avco Corp. Mod 7 silicone elastomer syntactic foam
11. Metal nose dome	Beryllium on flight model, 405 stainless steel on demonstration model for better thermal expansion match and reduced cost

A brief review of some of the selection criteria for each of the materials is perhaps apropos. Probably one of the most important general criteria is minimization of shrinkage. The dimensional tolerances quoted on Fig. 6 are more stringent than normally held on resin-fiberglass composites. To ensure as close a fit to these tolerances as possible, tool tolerances were held to <4 mills (compared with 10 mils shown on Fig. 6), and the tools were fabricated from 405 stainless steel, which has about the

(a) CRUSH OVERLAP

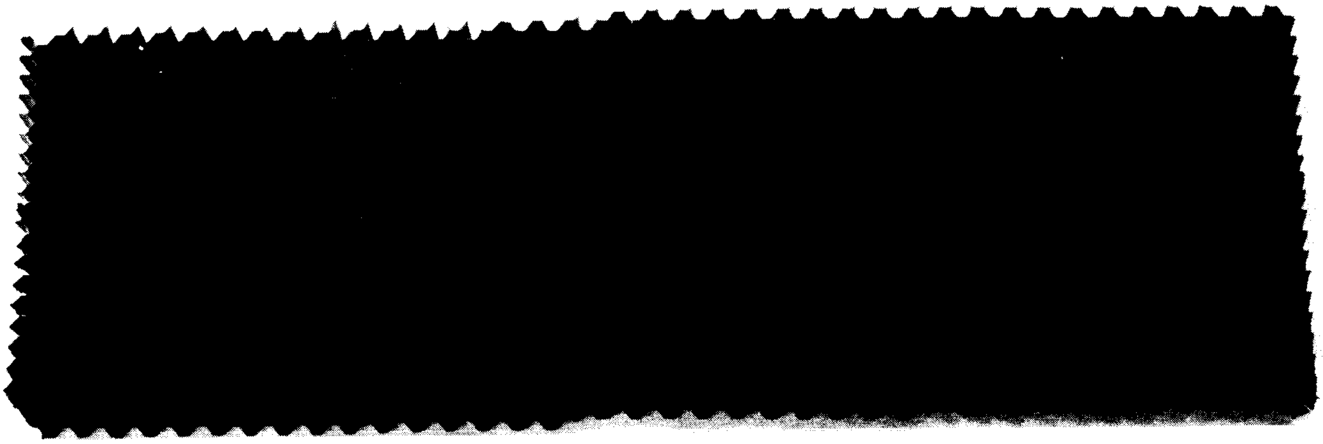

(b) FILM ADHESIVE

(c) FOAMING FILM ADHESIVE

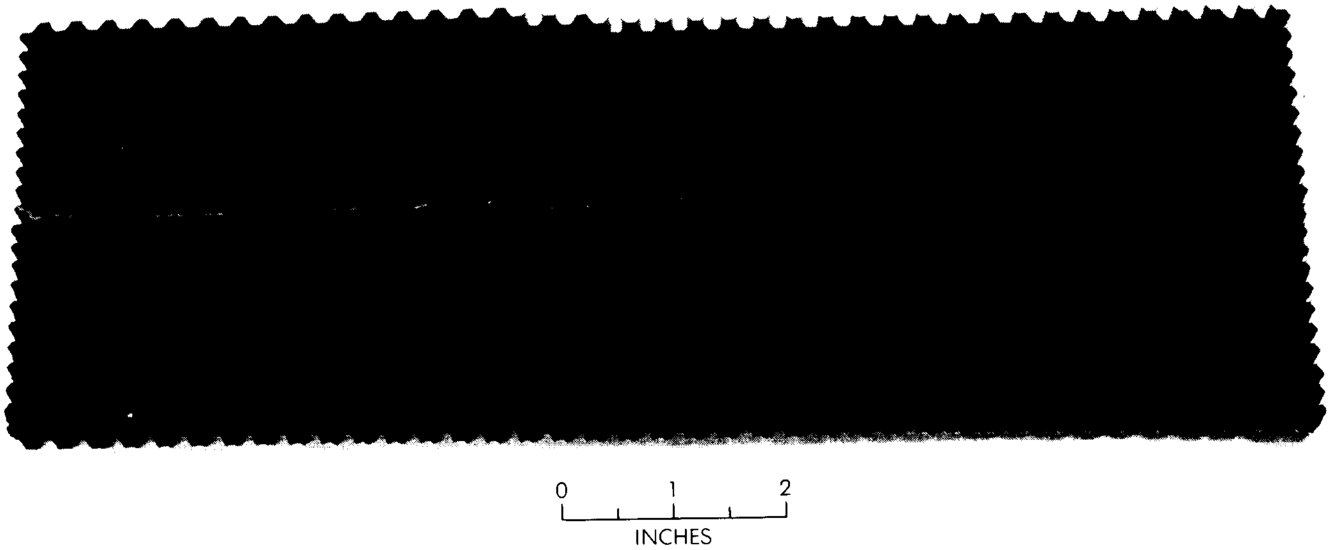

Fig. 5. Alternate core splicing techniques

FOLDOUT FRAME 1

FOLDOUT FRAME 2

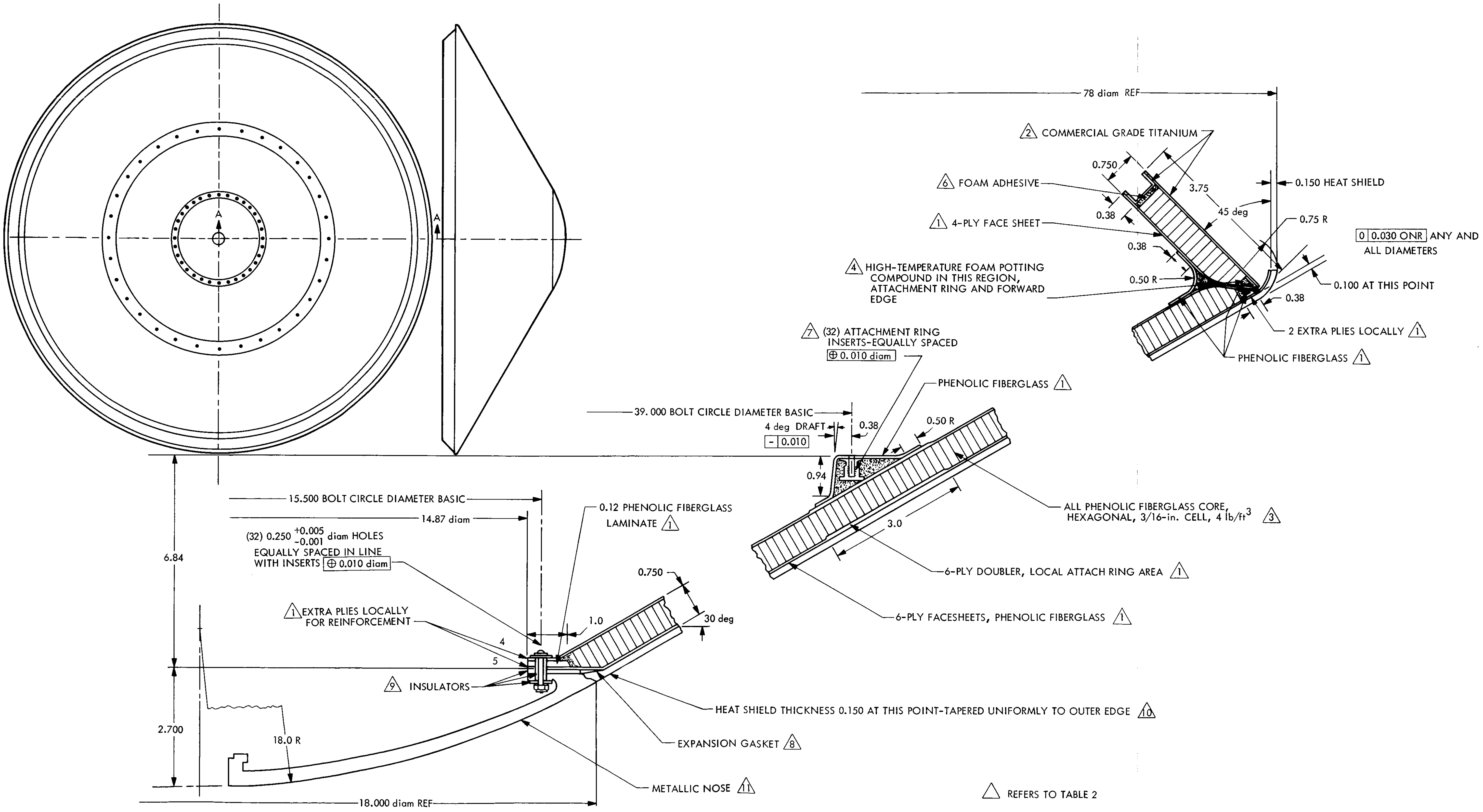
A
A
78 diam REF
2 COMMERCIAL GRADE TITANIUM
0.750
3.75
45 deg
0.150 HEAT SHIELD
6 FOAM ADHESIVE
0.38
0.75 R
1 4-PLY FACE SHEET
0 0.030 ONR ANY AND ALL DIAMETERS
0.38
4 HIGH-TEMPERATURE FOAM POTTING COMPOUND IN THIS REGION, ATTACHMENT RING AND FORWARD EDGE
0.50 R
0.100 AT THIS POINT
0.38
2 EXTRA PLIES LOCALLY 1
7 (32) ATTACHMENT RING INSERTS-EQUALLY SPACED
⊕ 0.010 diam
PHENOLIC FIBERGLASS 1
PHENOLIC FIBERGLASS 1
39.000 BOLT CIRCLE DIAMETER BASIC
4 deg DRAFT
- 0.010
0.38
0.50 R
0.94
ALL PHENOLIC FIBERGLASS CORE, HEXAGONAL, 3/16-in. CELL, 4 lb/ft³ 3
3.0
6-PLY DOUBLER, LOCAL ATTACH RING AREA 1
6-PLY FACESHEETS, PHENOLIC FIBERGLASS 1
15.500 BOLT CIRCLE DIAMETER BASIC
14.87 diam
(32) 0.250 +0.005 -0.001 diam HOLES EQUALLY SPACED IN LINE WITH INSERTS ⊕ 0.010 diam
0.12 PHENOLIC FIBERGLASS LAMINATE 1
6.84
0.750
30 deg
1.0
1 EXTRA PLIES LOCALLY FOR REINFORCEMENT
4
5
9 INSULATORS
HEAT SHIELD THICKNESS 0.150 AT THIS POINT-TAPERED UNIFORMLY TO OUTER EDGE 10
2.700
18.0 R
EXPANSION GASKET 8
METALLIC NOSE 11
18.000 diam REF
△ REFERS TO TABLE 2

Fig. 6. Schematic of aeroshell design for Mars probe

PRECEDING PAGE BLANK NOT FILMED.

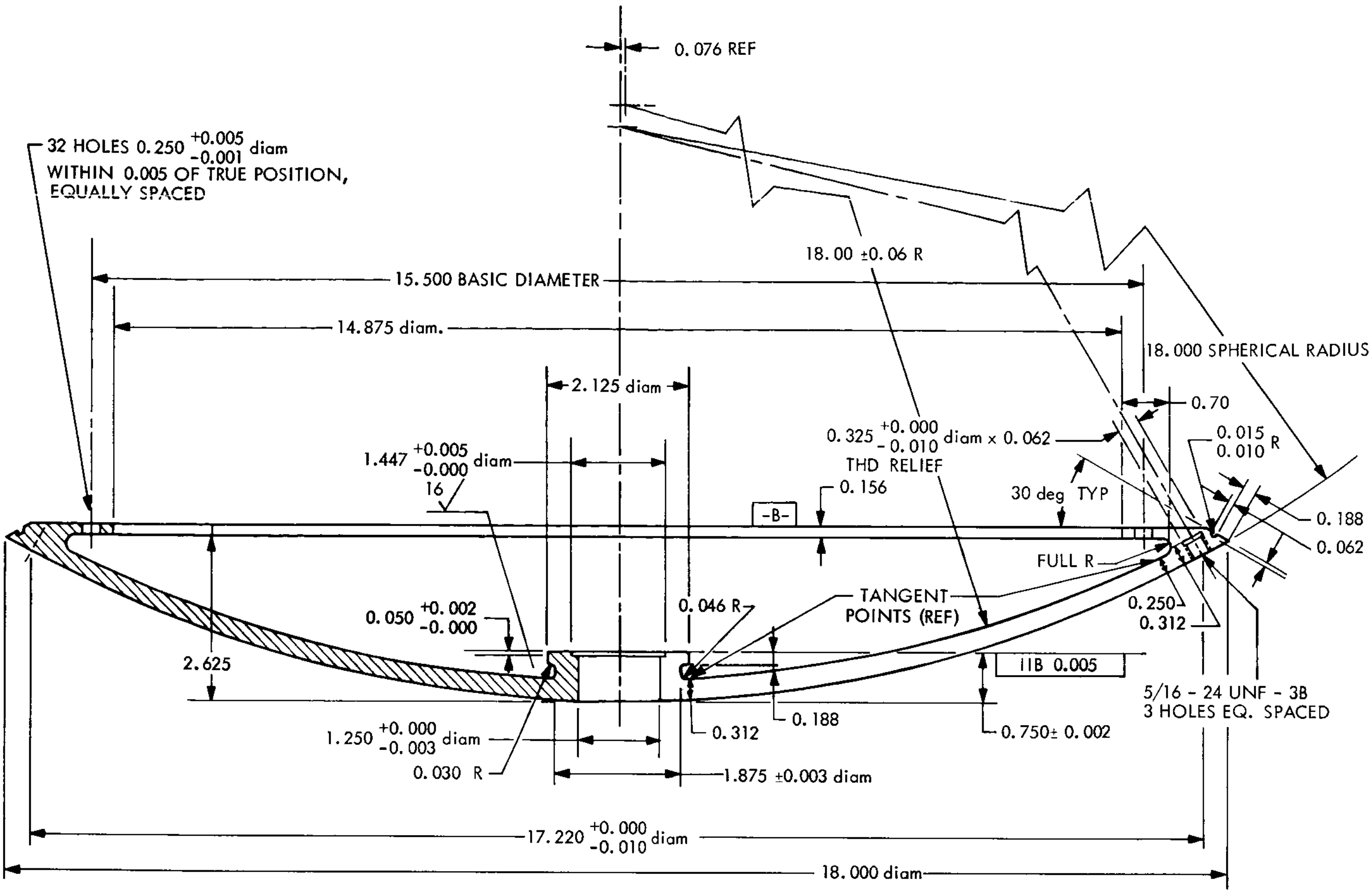
0.076 REF
32 HOLES 0.250 +0.005 -0.001 diam WITHIN 0.005 OF TRUE POSITION, EQUALLY SPACED
18.00 ±0.06 R
15.500 BASIC DIAMETER
14.875 diam.
18.000 SPHERICAL RADIUS
2.125 diam
0.70
0.015 0.010 R
1.447 +0.005 -0.000 diam
16
0.325 +0.000 -0.010 diam x 0.062 THD RELIEF
0.156
30 deg TYP
-B-
0.188
0.062
FULL R
0.050 +0.002 -0.000
0.046 R
TANGENT POINTS (REF)
0.250
0.312
2.625
IIB 0.005
5/16 - 24 UNF - 3B 3 HOLES EQ. SPACED
1.250 +0.000 -0.003 diam
0.312
0.188
0.750± 0.002
0.030 R
1.875 ±0.003 diam
17.220 +0.000 -0.010 diam
18.000 diam

Fig. 7. Beryllium nose dome detail

closest thermal expansion coefficient match of any metallic material suitable for tools (6.0 in./in./°F × 10^{-6} vs 5.5 in./in./°F × 10^{-6} for phenolic fiberglass).

The glass fabric and resin for the facesheet were primarily chosen from the earlier development program data and a constraint of a maximum heat-shield bondline temperature of 600°F. Style 112 E glass cloth was the lightest glass cloth tested with consistent strength and drape properties. The lightest cloth gives the most plies for the same required facesheet thickness and, thus, provides the greatest probability of reasonably isotropic properties in this small gage. The S glass was too expensive and difficult to weave; in addition, it was not generally available in cloths under 7 to 10 mils thick, so its additional strength could not be realized. Silane finishes did not appear to improve performance significantly in this particular use. The style 112 cloth with a plain weave was also used on the edge rings where the plies are aligned and forming characteristics over sharp radii were important. Style 181 cloth was used in the attachment ring for two reasons: isotropic strength properties were less critical and a considerable reduction in layup time could be accomplished. The forward reinforcement laminate was made from style 112 cloth, which provides a strong, dense, fine-textured laminate.

Only phenolic and polyimide resins, of those tested, perform well for short-time exposures of 600°F. Polyimide was more difficult to process during fabrication, and manufacturing controls on quality are not yet sufficiently established. The Adlock 851 was chosen over other B-stage phenolics primarily because it was the only one tested that met our requirements at the time the selection was made. Since then, several other phenolic resins have shown similar strength and handling properties. The amount of phenolic prepregged cloth that had to be returned to the manufacturer for not meeting a reasonably relaxed quality-control specification was surprisingly large. On the other hand, this appears to be typical of most of the prepreg suppliers.

The phenolic core was selected primarily because it was available at the time of decision and because it met the 600°F short-time performance criterion. Later examination of polyimide core did not show significant improvement. Molding of partially cured hexagonal core to complex shapes appears competitive with the built-in flexibility of other cell shapes. Molding the core while it is partially cured lessens cell distortion so that the greater strength of the hexagonal core (compared with the available selection of other core shapes in equivalent cell sizes) can be realized. Larger cell sizes are lighter in weight, but are also significantly weaker and do not meet the present design strength criterion. The larger the cell size the greater the probability of local buckling of the thin facesheets across the cell gap. The core thickness was chosen somewhat arbitrarily. Later tests showed that ¾ in. thick and ½ in. thick core gave similar performance, but 1 in. thick core appeared significantly weaker.

The aft cone acts primarily as a stiffener. Modulus, rather than strength, is important. Titanium was chosen as the basic stiffening agent, not only because it has a higher modulus-to-weight ratio than fiberglass, but because its thermal expansion coefficient is one of the few that closely approximates the expansion coefficient for phenolic fiberglass. This expansion match makes composite fabrication attractive. Since strength is of secondary importance, commercially pure titanium was used. Commercially pure titanium has about the same modulus as other titanium alloys, but its lower strength makes it much easier to fabricate in such complex shapes as the U ring. Also, it may be hot-sized with applied heat, thus eliminating investment in high-tolerance, complicated, and expensive hot sizing tools. The fiberglass core saves weight, and the inner skin need only be strong enough to hold the sandwich structure together under the anticipated loads. The aft cone is sized by moment-of-inertia considerations which require the backward projection in mass. The aft cone is stepped from the outer edge to prevent wake reattachment during flight with a subsequent order-of-magnitude increase in local heat load.

The fiberglass rings at the outer edge are primarily tie-ins between the two cones. They are used to link the facesheets of the two cones. These rings also contribute to the hoop strength at the edge. The rings are fiberglass since strength, rather than modulus, is important. The adhesive is also more compatible with the primarily fiberglass structure. Local potting at the joint is mostly for shape retention, so that transfer of stress between the facesheets will not be degraded by misalignment. This is the same potting compound used elsewhere in the structure.

The extended aft edge is structurally compatible with the anticipated loads without additional reinforcement (other than the two extra facesheet plies). It is also important to prevent wake reattachment, as mentioned earlier.

The attachment ring is the primary load-transferring position between the structure and the payload. The distributed pressure load during entry causes a moment force on both sides of the joint and the aerodynamically induced stresses are maximized at this region. A 6-ply doubler is used in this area to increase the local strength. The style 112 cloth permits imperceptible fairing of the doubler into the continuous skin. The thickness of the attachment ring skin is primarily determined by a buckling calculation on the 0.94-in. vertical span without the supporting potting compound on one side. The potting compound was formulated for this program. Although the density (31.2 lb/ft^3) is low, the compression strength of the syntactic foam is around 5000 psi. The epoxy used in the formulation will take 500°F for short times. It is not expected that the potting compound will see temperatures in the range of 500°F here or at other locations, except when the stress loads are either small or nonexistent.

In the forward area of the cone, the extra facesheet plies, the reinforcement laminate, and the small amount of epoxy foam potting compound act both to tie in the facesheets and to reinforce the joint against local moments caused by differential expansion of the beryllium nose and the fiberglass. Differential expansion is also allowed in the expansion gasket and in the heat shield–beryllium joint. Tests are planned to determine if there is a peel problem between the heat shield and the structure at the heat shield–structure–gasket interface. If so, an extra ply with loops sticking up into the ablator can be added to prevent peel propagation. This use will be shown later.

The adhesive between the facesheets and core is one ply of 0.03 lb/ft^2 FM96U, a high-temperature epoxy adhesive in the form of an unsupported film, 4 mils thick. In local regions near joggles (e.g., at the edges of the attachment ring doubler and the front edge of the core), a second layer of FM96U is applied. Two layers of this same film adhesive are required at the titanium–core interface to ensure a proper bond. Supported FM96 adhesive film (0.06 lb/ft^2) is used locally at the interface of the two cones to allow for variations in gap mismatch. Epoxy foam adhesive FM40 is used between the core and the titanium U-ring on the aft cone to ensure good bond contact.

The flight dome is designed in beryllium to provide the most efficient metallic heat sink. A heat sink capability is needed to allow gas cap radiation measurements at the nose for Mars atmospheric composition determinations without bias from ablation products. Since damping of the flight vehicle's angle-of-attack variation about the flight path is not well understood, it is difficult to place a specific limit on the variation of the stagnation point about the nose tip. Partly as a conservative estimate of stagnation point variation and partly for ease of fabrication, it was decided that the entire spherical portion of the nose would be metallic heat sink and would be faired into the cone at the tangent point. In order to get the shock layer standoff distance sufficiently large during anticipated Mars entry conditions so that the radiation signal would be large enough for instrument discrimination, it was necessary to make the nose radius at least 18 in. For vehicle stability reasons the 18-in. lower limit was chosen. The hole at the nose accommodates the radiometer. Several other holes (not shown) are anticipated about halfway between the centerline and the joint, which would accommodate atmospheric sampling devices for gas chromatography and mass spectrometer backup experiments for atmospheric composition determinations. The beryllium nose weighs under 6 lb. The demonstration model shown later in this report is made from 405 stainless steel partly from cost reasons and partly for thermal expansion match during early structural tests. The beryllium nose for flight is designed to reach a maximum temperature of 1200°F.

The insulators at the metal nose–fiberglass structure interface have to withstand short-time temperatures in flight up to 1200°F. To meet this constraint, low-density (less than 25 lb/ft^3) sintered silica fibers in a nonfriable form were selected. This material has both a low conductivity (approximately 2×10^{-5} Btu/ft^2 s) and a reasonable compressive strength (100 psi or better).[1] Preliminary tests indicate that the material does not disintegrate under anticipated launch vibrations. Phenolic fiberglass insulators were used in the demonstration model to limit costs.

The ablator (Avco Mod 7) is a methylphenyl silicone elastomer filled with phenolic microballoons and glass fiber. Bond compatibility between the silicone elastomer and the phenolic surface is good, partly because the porous fiberglass surface provides a mechanical bond. The elastomer is applied by a roller, similar to painting a wall in a somewhat dry form; it is then cured under vacuum bag conditions. Roller coating and vacuum bagging were chosen over other application and curing forms because of ease of fabrication and because 80 to 90% of the mechanical properties under optimized molding conditions are achieved. Additionally, this type of elastomer is also easy to repair. Choice of this particular elastomer was primarily based on convenience and price. A number of other manufacturers have heat shield materials with equivalent ablation response in the Mars direct entry regime and with varying amounts of fabricability data. Preliminary test programs within NASA tend to indicate that simple modifications in any of these materials could halve the amount of heat shield needed for an actual mission. This particular material was available and, in the quantities indicated, allows a meaningful payload and mission.

B. Tooling

A schematic of the major bond tools is shown in Fig. 8. The major tools are the two conical bond jigs for the fore and aft cones and the central spider. All of these tools are made of 405 stainless steel for thermal expansion coefficient match with the part and provide a factor of 3 or better in tolerances over those tolerances listed in Fig. 6. The tools are made very heavy to minimize thermal-cycle distortion. The major bond jig for the large cone (see Fig. 9a) acts as a layup fixture and centers the cone to a true centerline through the bushed center post hole. The aft bond jig for the smaller cone also acts as a layup fixture and centers the aft cone about the same centerline through the central spider tool. The aft bond jig also has titanium U-ring clamping fixtures, which will be shown later. The two bond jigs mate up with matching parallel planes so that they may be shimmed to provide any desired gap between the faying surfaces of the two major conical parts. Figure 9b shows the two bond jigs mated together.

The central spider is keyed to its main centerpost. The centerpost and the adjustable arms on the spider center the two conical bond jigs. The attachment ring fixture is built into the spider and is keyed to the same centerline. Bushings in the attachment ring fixture and at a forward extension of the spider locate the ring hole patterns to the same centerline. The central spider is, thus, a centering fixture, an attachment ring layup fixture, and drill fixture for both bolt circles.

Later work in the program added several supplementary tools to the major tool system. Drilling the forward

---

[1] Tellep, D. M., Lockheed Missiles and Space Company, personal communication, December 6, 1965.

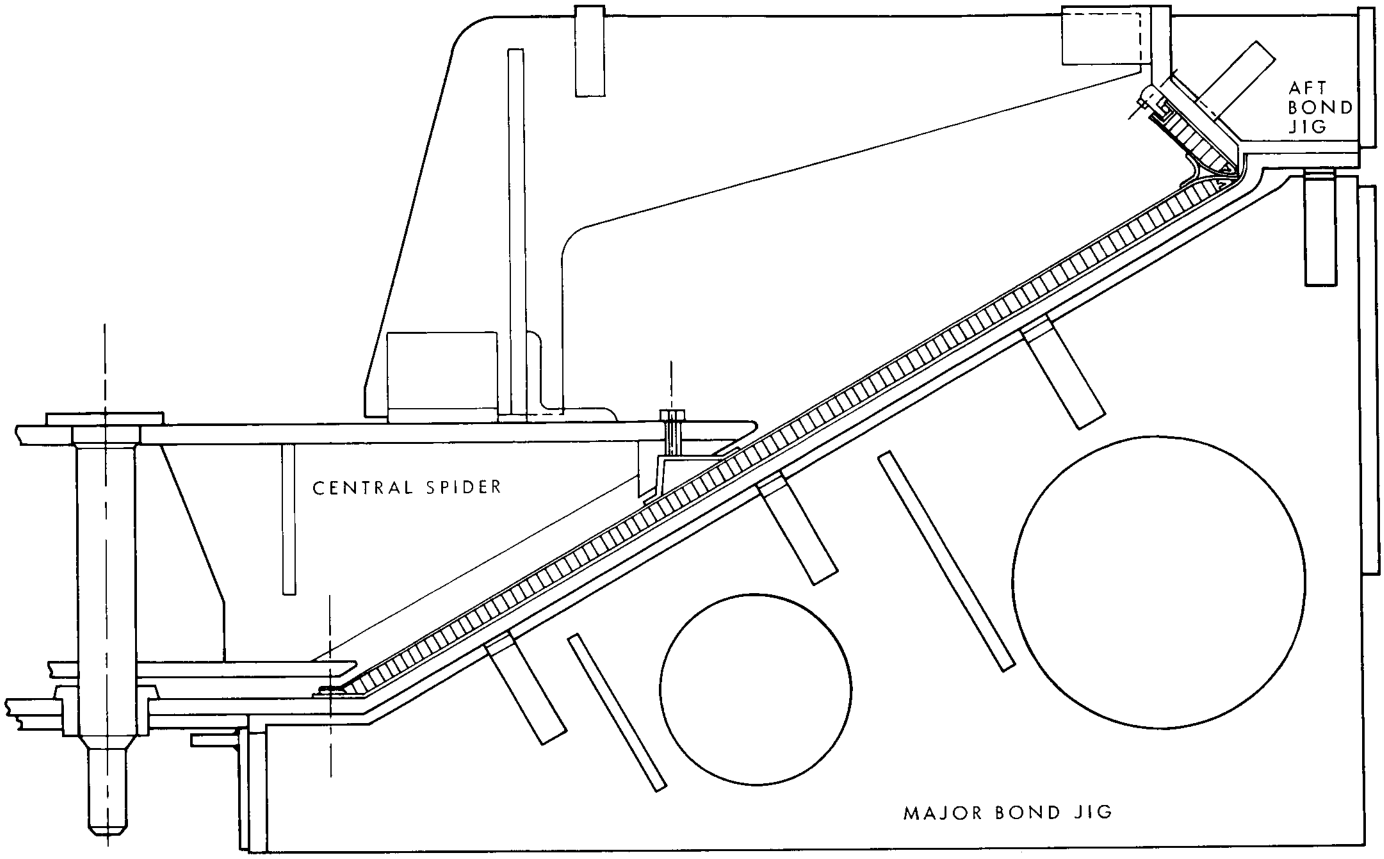
AFT BOND JIG
CENTRAL SPIDER
MAJOR BOND JIG

Fig. 8. Schematic of major tool assembly

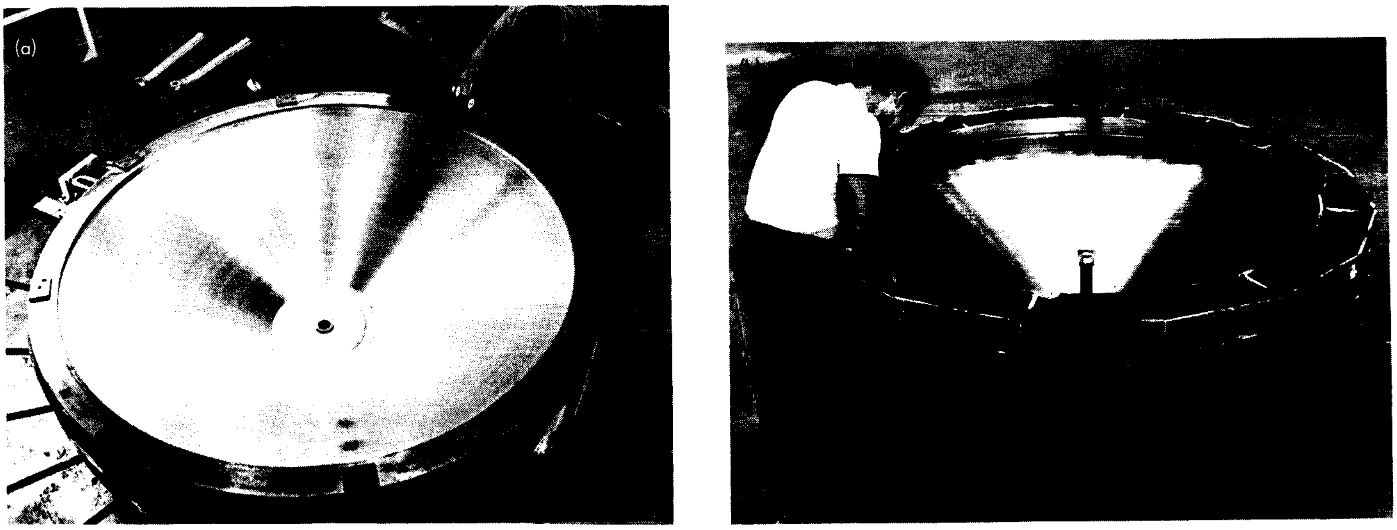

Fig. 9. Major bond jigs

bolt circle from the inside position was difficult and reduced accuracy, so a second plate was developed for drilling the bolt circle from the front of the major cone. The bushed holes in the second plate were keyed to the original plate in the central spider so that positional location remained within 3 mils. It was also established that the forward joint would be flatter and have a smoother break between the flat and the cone if a pressure plate were used, both in the spacer or laminate bonding and in curing the second facesheet. These tools were constructed and used for the second aeroshell.

Numerous templates were made for cutting, routing, and locating the facing plies and the core. A plaster cone was constructed both as a welding tool in making the major bond jig and as a core forming tool. The remaining tools are primarily for the titanium parts. A breakforming jig was constructed to form the titanium into a channel. Channel U-angle, about ⅓ the total ring dimension, were then stretch-formed about a curved tool to the 45-deg U-angle with a flexible metal spider in the U of the channel to maintain its basic rectangular shape. These tools are shown later in the detailed part fabrication. Welding jigs were fabricated to join the titanium parts.

III. Detail Fabrication of Basic Cone

The aeroshell fabrication specification or outline used to make the 6½-ft-diam aeroshells is included as the Appendix. More detailed fabrication sheets were made for each detail part or assembly for use by the technicians. This report provides a pictorial outline of the actual fabrication. Emphasis is on particular portions of the fabrication that are felt to be typical, difficult, and interesting. Repair techniques for real or potential errors are discussed in Section VII.

A. Detail Parts

A grouping of sections of all the major detail parts is shown in Fig. 10. The titanium U-ring is shown at the top. One fiberglass V-ring and the C-ring are shown in the center with the V-ring already prepotted. The attachment ring skin is shown with the metal inserts in place. The fiberglass disk lies in the foreground.

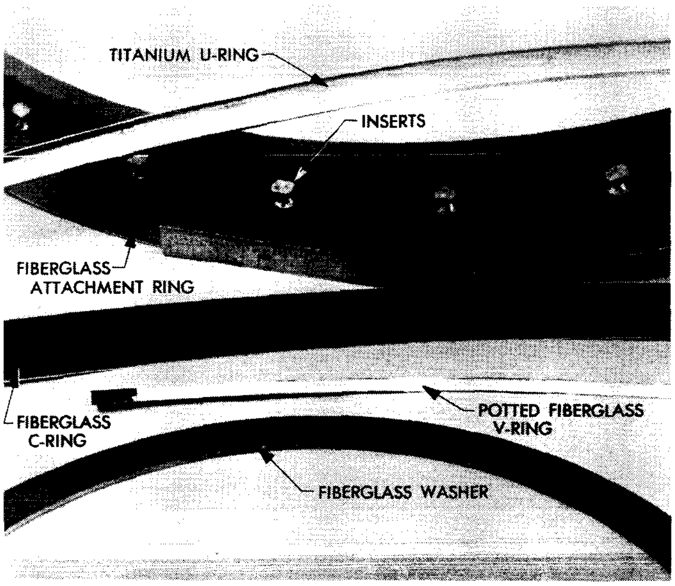

Fig. 10. Closeup of detail parts

The titanium part fabrication is reasonably straightforward. Templates are used to cut commercially pure titanium pieces from sheet stock; 20-mil pieces are breakformed into channel. The channels are then stretch-formed as shown in Fig. 11 into approximately ⅓-circumference U-rings at a 45-deg angle to the hoop centerline. A flexible metal spider is used to hold the U shape during the stretch-forming operation. The 120-deg segments are then annealed and reformed in the same tool. The ends of the three partial rings are trimmed to remove distorted areas and are then tungsten-inert-gas (TIG) welded in special fixtures to reduce the possibility of misalignment with the aft cone bond tool. The three facesheet pieces are similarly welded, and fit to the aft cone bond tool is rechecked after each weld. Since only vacuum pressure is used in bonding, the detail titanium parts must fit exactly to the bond tool.

The V- and C-rings for reinforcing the joint between the two cones are made in halves. Seven plies of impregnated 112 cloth are stretched and formed over a male tool, inch by inch, to ensure no wrinkles in the final ring. The warp of each ply is aligned circumferentially. The halves are vacuum-bagged and cured at 50 psi (by use of supplementary autoclave pressure) for ½ h at 300°F and 2 h at 350°F. Quality assurance samples of 8-ply laminate taken from the same impregnated cloth batch accompany each cure; these are tested and compared against earlier data. The half-rings are then trimmed to size and are rejected if wrinkles remain after trimming. The V-rings are potted with the epoxy foam (see Table 2) except in the local region where the final splices will be. The potting compound is cured under vacuum-bag pressure for 1 h at 350°F. The V-ring is pre-potted to ensure

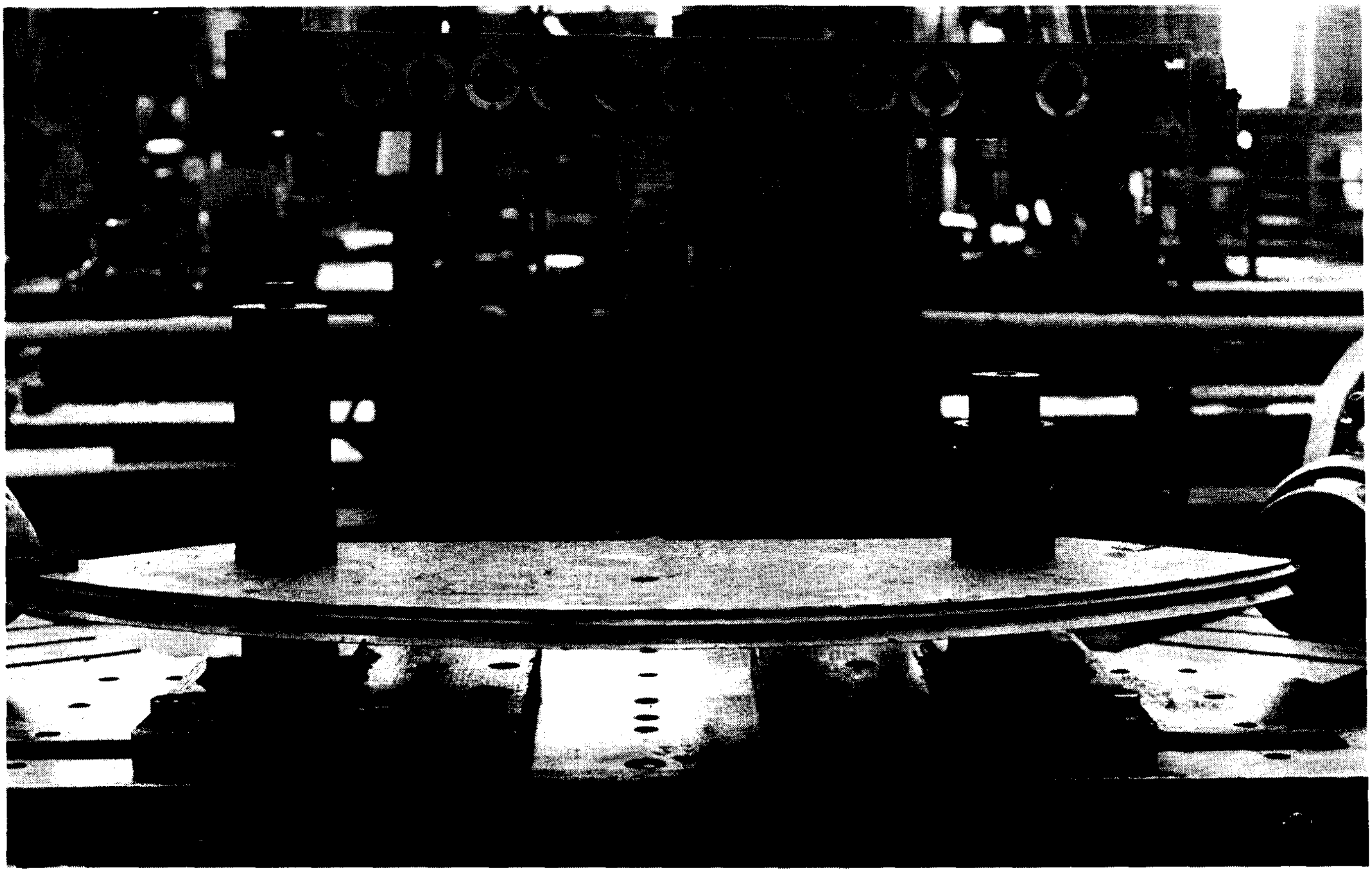

Fig. 11. Stretchforming setup

retention of the V angle during subassembly later in the fabrication.

The attachment ring is layed up in the central spider. Precut circular segments of approximately 90 deg are layed up with ¼-in. overlaps. Each ply is rotated 45 deg from the one before. Two plies of prepregged 112 cloth are layed up next to the tool to provide a smooth finish. Five plies of 181 cloth are added to bring the nested thickness to about 50 mils. Five plies of 181 cloth appear to give the same strength as an equivalent thickness made with 112 cloth but layup time is reduced considerably. A special cure is used on the attachment-ring laminate. The vacuum-bagged part is given a supplementary pressure of 50 psi at 215°F in an autoclave to ensure proper resin flow into the bends of the layup. Pressure is then reduced to vacuum-bag pressure, alone, and the temperature stepped for ½ h at 275°F, ½ h at 300°F and 2 h at 350°F. If pressure is applied for the full cure to ensure a dense laminate, shrinkage is excessive. After curing, the laminate is inspected for proper release from the tool before proceeding. Thirty-two holes are machined in the refitted skin through the bushings used for insert location.

The laminated fiberglass spacer between the facesheets at the fore end of the main cone is made from 15 plies of phenolic-impregnated 181 cloth. The plies are layed up in a large square laminate with each ply rotated 45 deg from the previous. After curing, the part under vacuum-bag conditions for ½ h at 300°F and 2 h at 350°F, the part is machined into a 0.125-in.-thick disk per Fig. 6.

The major insulator between the structure and the metallic dome is also machined to dimension per Fig. 6. If it is the flight model, the insulators are all sintered silica fiber foam (Table 2). For the demonstration model, the flat major insulator is a 10-ply laminate, similar to the 15-ply spacer, which is then machined to a 0.075-in. thickness. The bolt insulators and washers are machined from standard high-temperature phenolic-fiberglass stock laminates.

B. Aft Cone Assembly

The titanium parts are phosphate fluoride cleaned just before aft cone assembly. The prefitted and welded 0.015-in. titanium facesheet is refitted to the aft cone. In the first aeroshell, this skin was joined by adhesive bonding with 1-in. doublers, rather than by welding. Improved welding techniques allowed elimination of the extra doubler weight in the second aeroshell. Two plies of the epoxy film adhesive (see Table 2) were applied over the full facesheet surface. The U-ring is then layed in place and clamped tightly, as shown schematically in Fig. 12. The metal finger and rubber pressure pad hold the U-ring tightly against the facesheet with the faying surface parallel.

Three precured, honeycomb-gore segments are cut and fit against the adhesive. The gores are overlap-spliced. Although it would be structurally better to have the core ribbon in the circumferential or hoop direction, the ribbon direction had to be placed in the radial direction to lessen the chance of core crushing during vacuum-bagging. Even so, a copper hoop had to be used to prevent lateral crushing. Potting compound could have been used to prevent this, but the accompanying increase in weight was not desirable. The epoxy foam adhesive (Table 2) is applied as a film between the end of the core and the titanium U-ring. This subassembly is then vacuum-bagged and cured 1 h at 350°F. The curvature on the forward end of the core must now be machined and the thickness of the core must be machined flush with the U-ring.

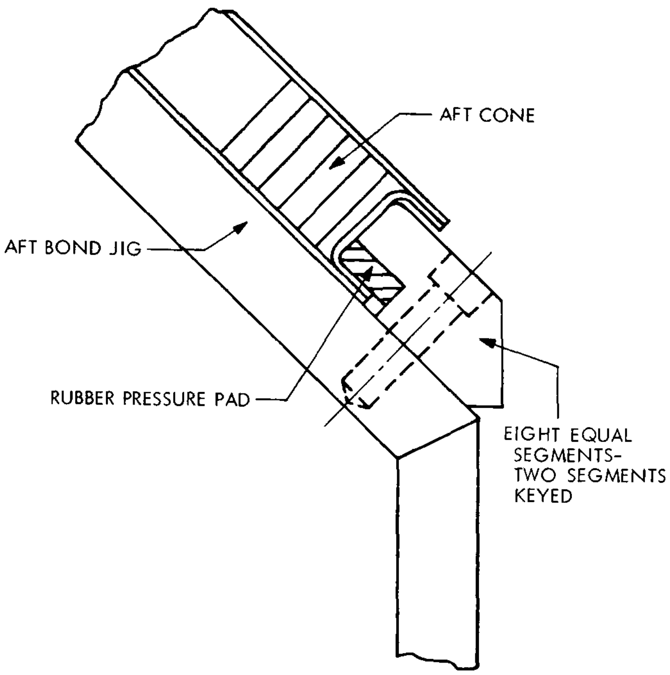

Fig. 12. Schematic of titanium part clamping arrangement

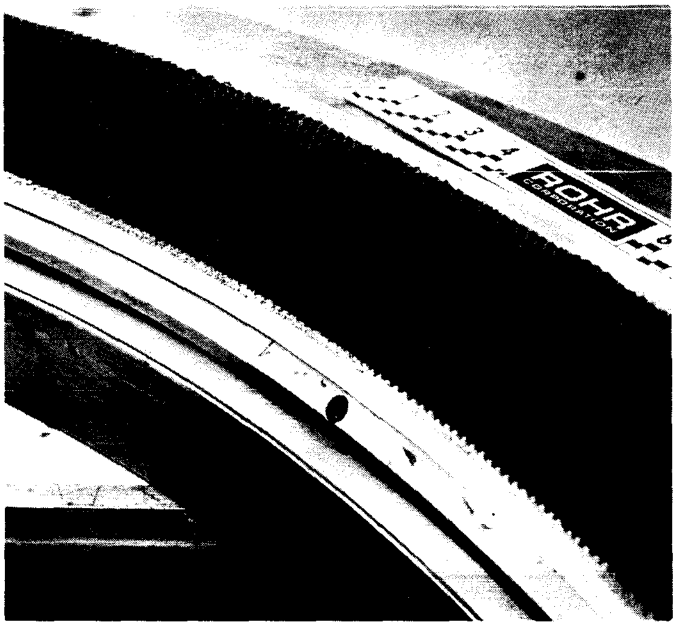

Fig. 13. Aft cone assembly after first cure and with the core machined

A photograph of the part at this stage is shown in Fig. 13. To save weight, the cell walls in the regions immediately adjacent to the position for the V-ring must be sealed with a minimum amount of room-temperature-curing epoxy to prevent the epoxy foam potting compound from filling cells other than those along the immediate periphery. The V-ring must be recleaned in the area where the new adhesive will be applied. The potted aft cone half V-rings can now be placed in position with 1-in. doublers joining them (see Fig. 14). Epoxy foam is added to the region to fill existing gaps (see Fig. 15). One ply of the film adhesive is then layed up over the V-ring, foam, core, and titanium V-ring, followed by 4 plies of the standard 112 cloth. After trimming the skin to the U-ring, the entire aft cone is vacuum-bagged and cured for ½ h at 300°F and 2 h at 350°F. The cured skin has a fine, dry texture and is slightly dimpled (Fig. 16). The finished 6-ft conical aft stiffening ring is very light (approximately 5.9 lb) and can easily be held in one hand (Fig. 17).

C. Major Cone Assembly

The outer facesheet of the major cone may now be layed up in the major bond jig using 6 plies of phenolic

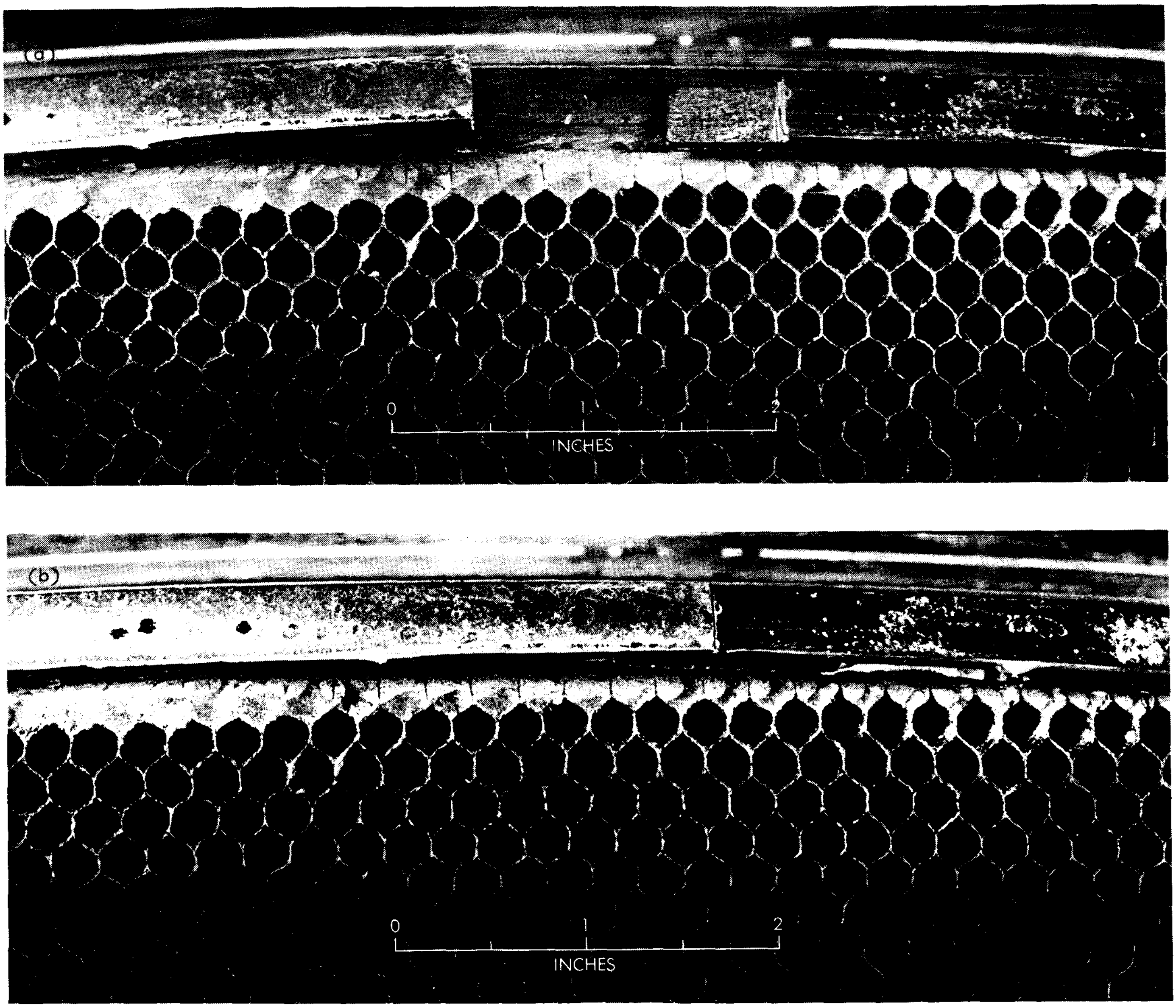

Fig. 14. V-ring splice

impregnated 112 cloth (Table 2) and local doublers at the forward and aft regions and in the attachment ring area (see layup process in Fig. 18). The warp direction of each ply is again rotated 45 deg from the previous ply, and the individual gore segments are overlapped ¼ in. The phenolic fiberglass spacer is centered at the front end of the cone with one layer of the epoxy film adhesive between it and the facesheet. A metal ring pressure plate is placed on the spacer ring to reduce the possibility of voids at the 30-deg transition. After vacuum-bag curing for ½ h at 300°F and 2 h at 350°F, the facesheet may be removed from the tool and handled as a reasonably stiff free-standing shape (Fig. 19). An advised precaution is to reinforce the aft edge of the skin with copper tubing prior to removal from the tool to protect the outer curvature.

In the meantime, partially cured hexagonal core (Table 2) is cut into gore segments and conformed to shape on a plaster tool. A heat gun is then used to advance the cure sufficiently to hold the shape (Fig. 20). The core is again overlap-spliced on the same tool (Fig. 21) with a minimum 1-cell, maximum 2-cell overlap. The forward edge of the core is then machined and

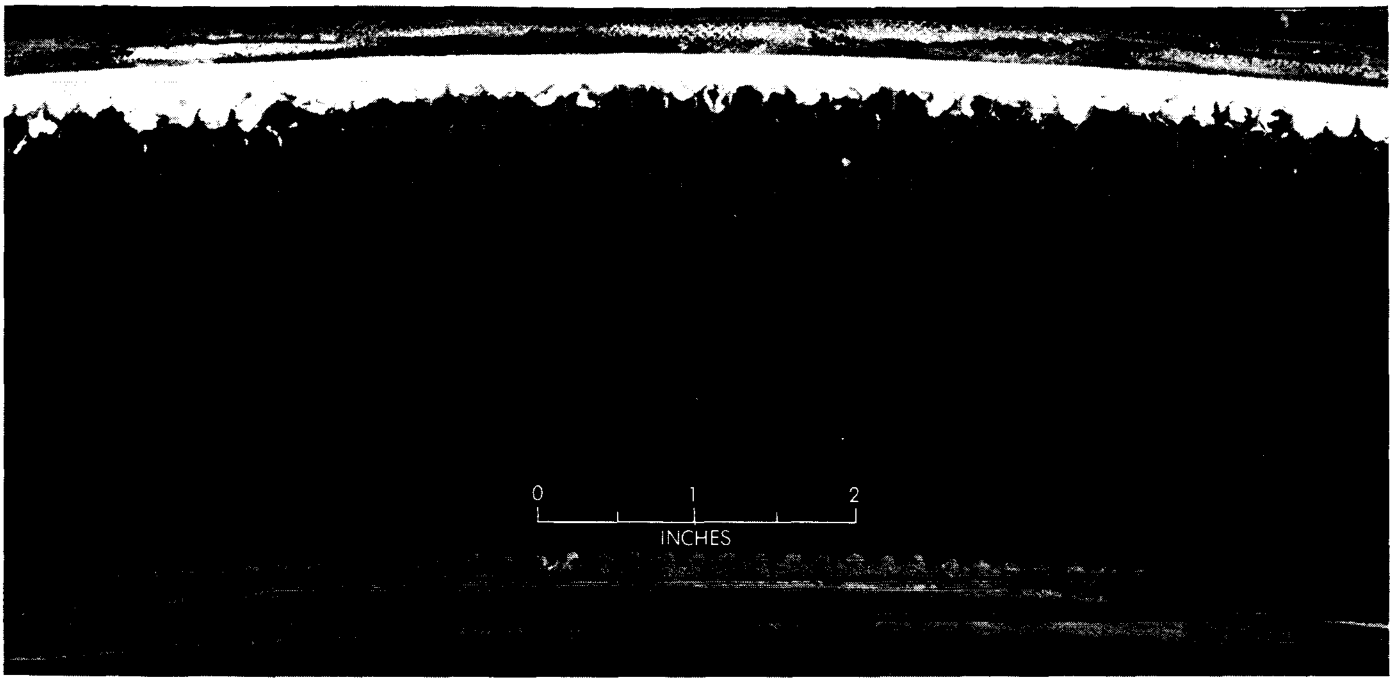

Fig. 15. V-ring and potting compound in place

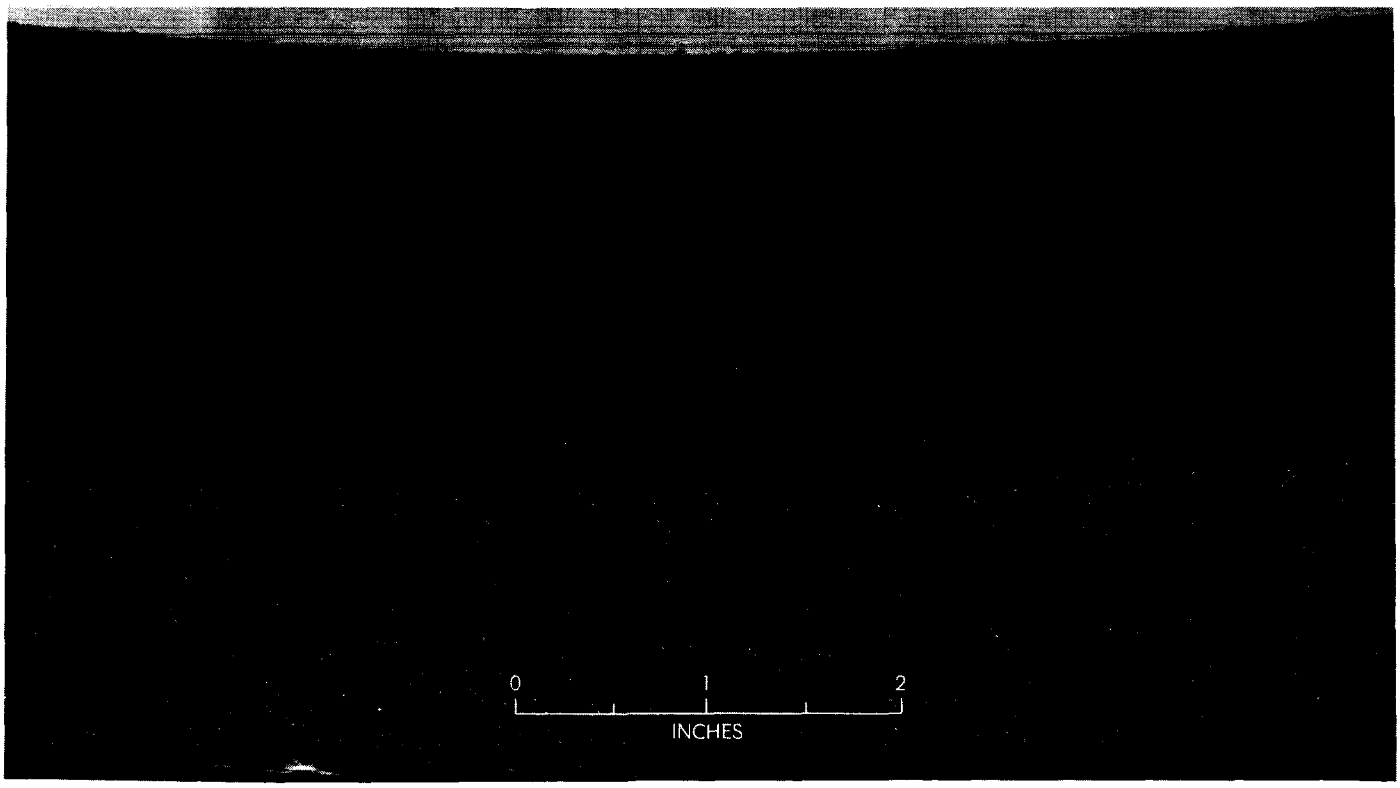

Fig. 16. Texture of 4-ply phenolic-fiberglass facesheet on aft stiffening cone

fit to the outer facesheet. One ply of the epoxy film is applied over the entire inner surface of the first facesheet, except at the outer curvature. Additional plies of adhesive are applied at critical regions at the fore end of the cone and at the doubler joggles. The core is then positioned in place and the epoxy potting compound is applied at the forward edge of the core. The entire assembly is vacuum-bagged and cured for 1 h at 350°F. A pressure plate is again used at the forward surface to ensure a flat surface. At this stage, the bond between the core and the first facesheet is inspected, and the assembly looks as shown in Fig. 22. The core may now be machined at the aft edge with the attachment ring tool

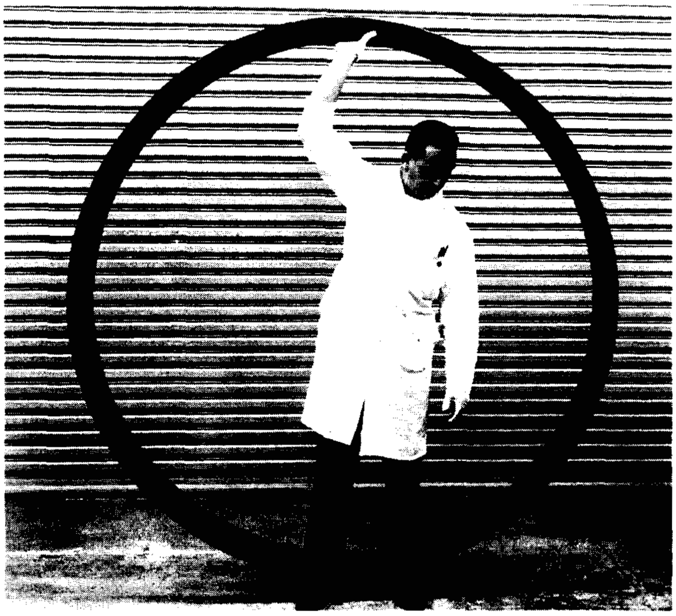

Fig. 17. Completed aft stiffening cone

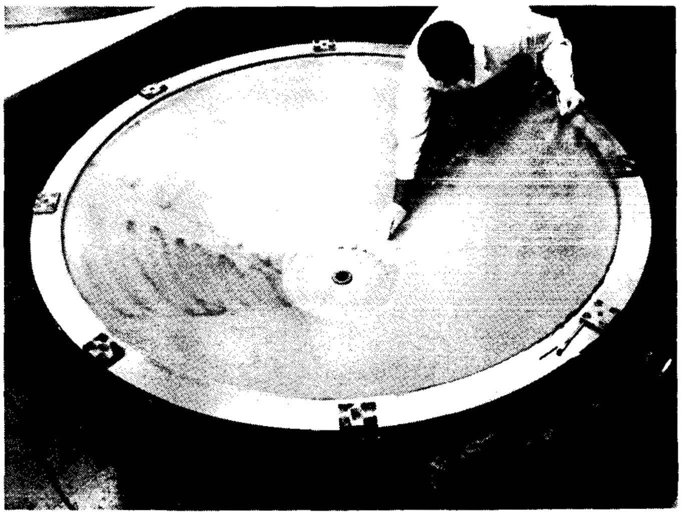

Fig. 18. Laying up first facesheet on major cone

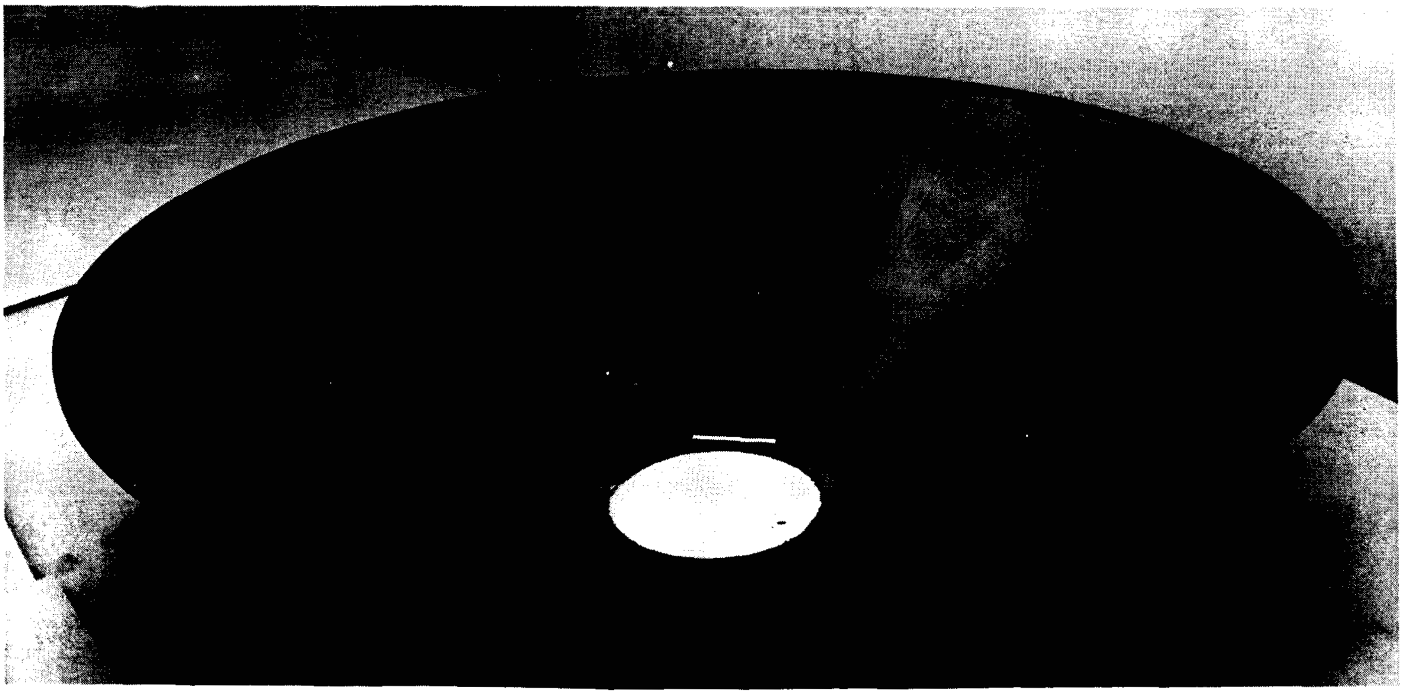

Fig. 19. Outer facesheet on major cone, freestanding

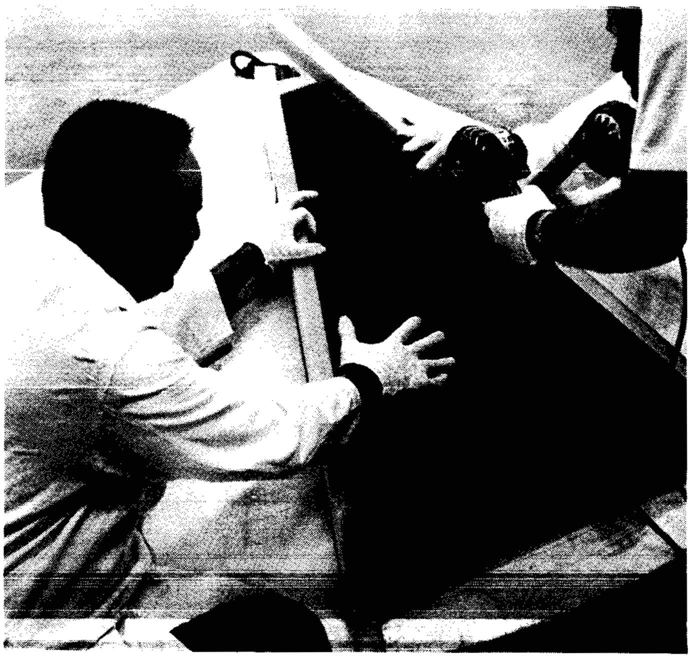

Fig. 20. Forming honeycomb core for major cone

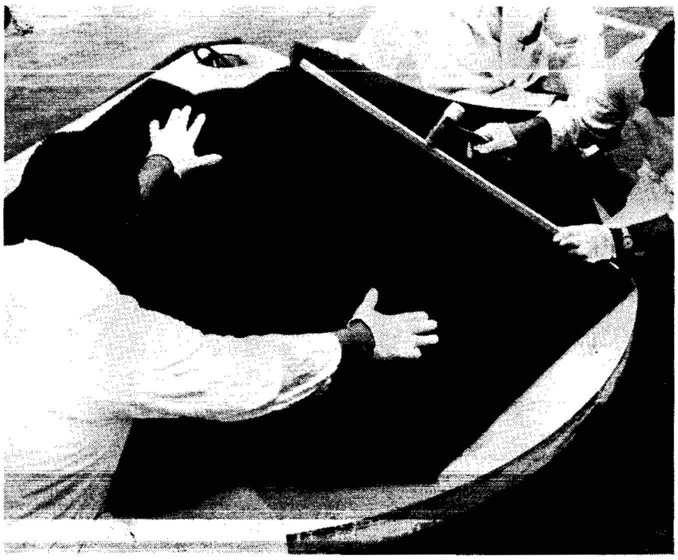

Fig. 21. Splicing honeycomb core for major cone

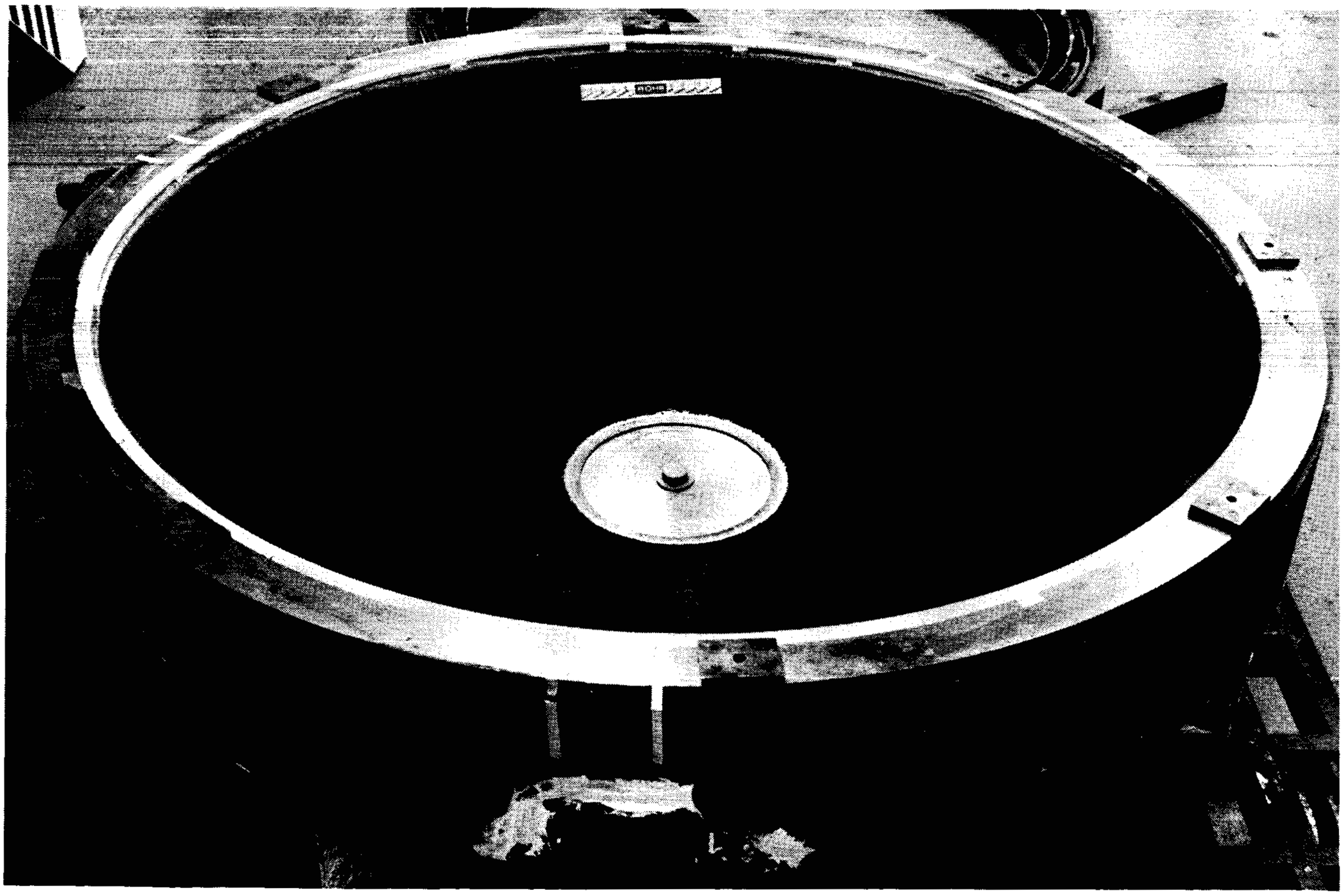

Fig. 22. Major cone with core cured in place

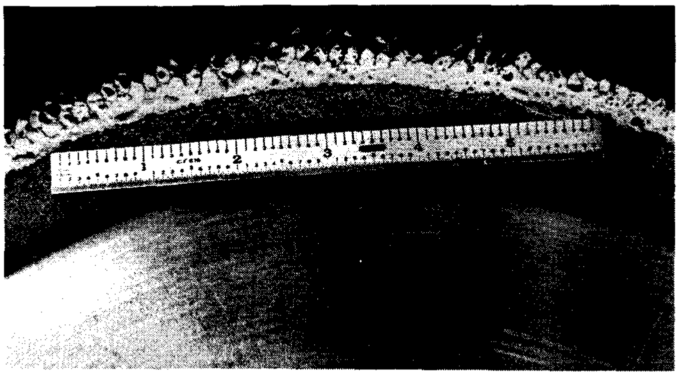

Fig. 23. Machined surface at forward ring

as an extra hold-down tool to prevent rotation in the tool. A full machine cut using a coordinated profile template may then be taken along the cone to mate the cone and potting compound smoothly to the forward end (Fig. 23). The cone edges must again be sealed with a room temperature epoxy sealant in the region near the second V-ring. The V-ring halves may then be layed in place, spliced with 1-in. doublers, and potted with the lightweight epoxy foam (Fig. 24).

The second facesheet may now be layed up on the core. One layer of the film adhesive is layed up over the entire area with a second layer locally at the forward end of the cone. The facesheet is 6 plies of phenolic impregnated 112 cloth with a 6-ply doubler on the outside at the attachment ring area and 4 extra plies at the forward end. It is layed up in eight gore segments overlapped ¼ in. (Fig. 25). Each ply has the warp direction

Fig. 25. Laying up second facesheet on major cone

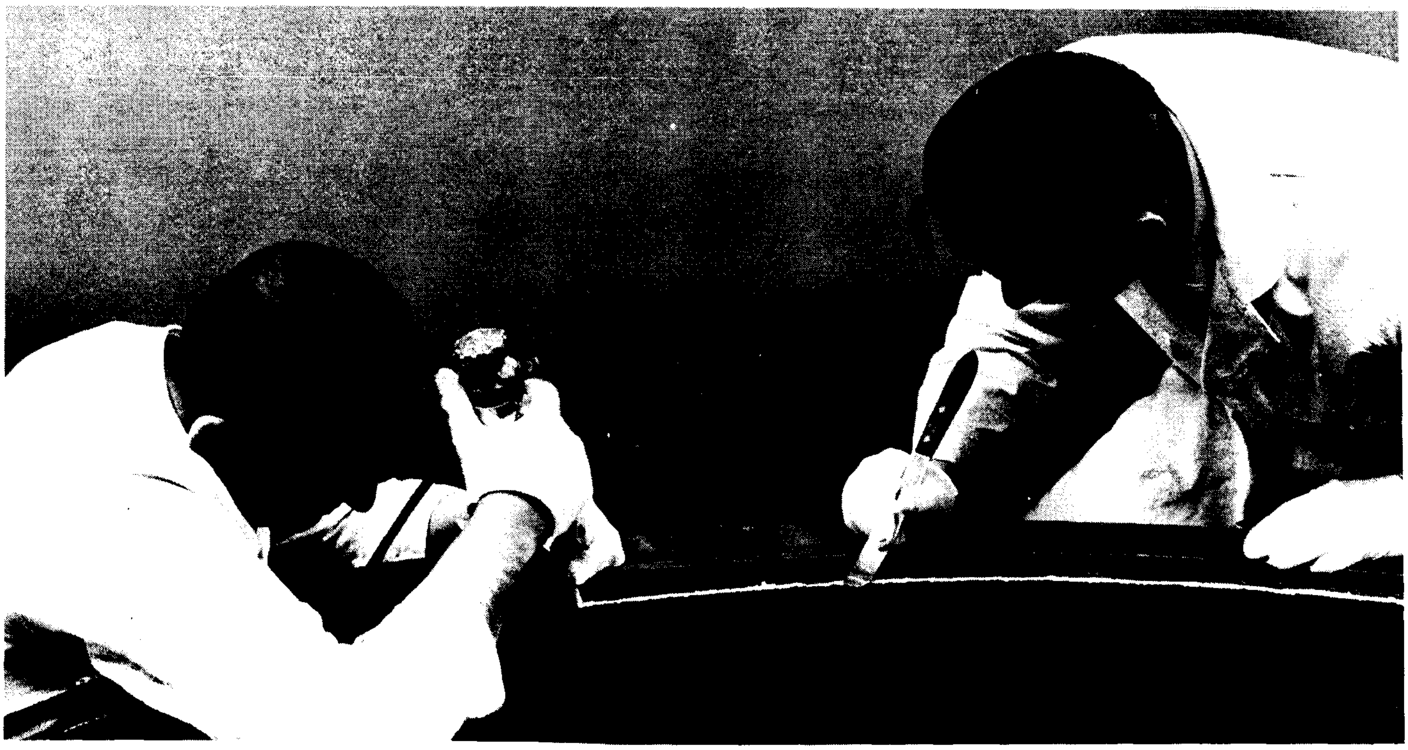

Fig. 24. Potting lightweight epoxy foam at V-ring locations

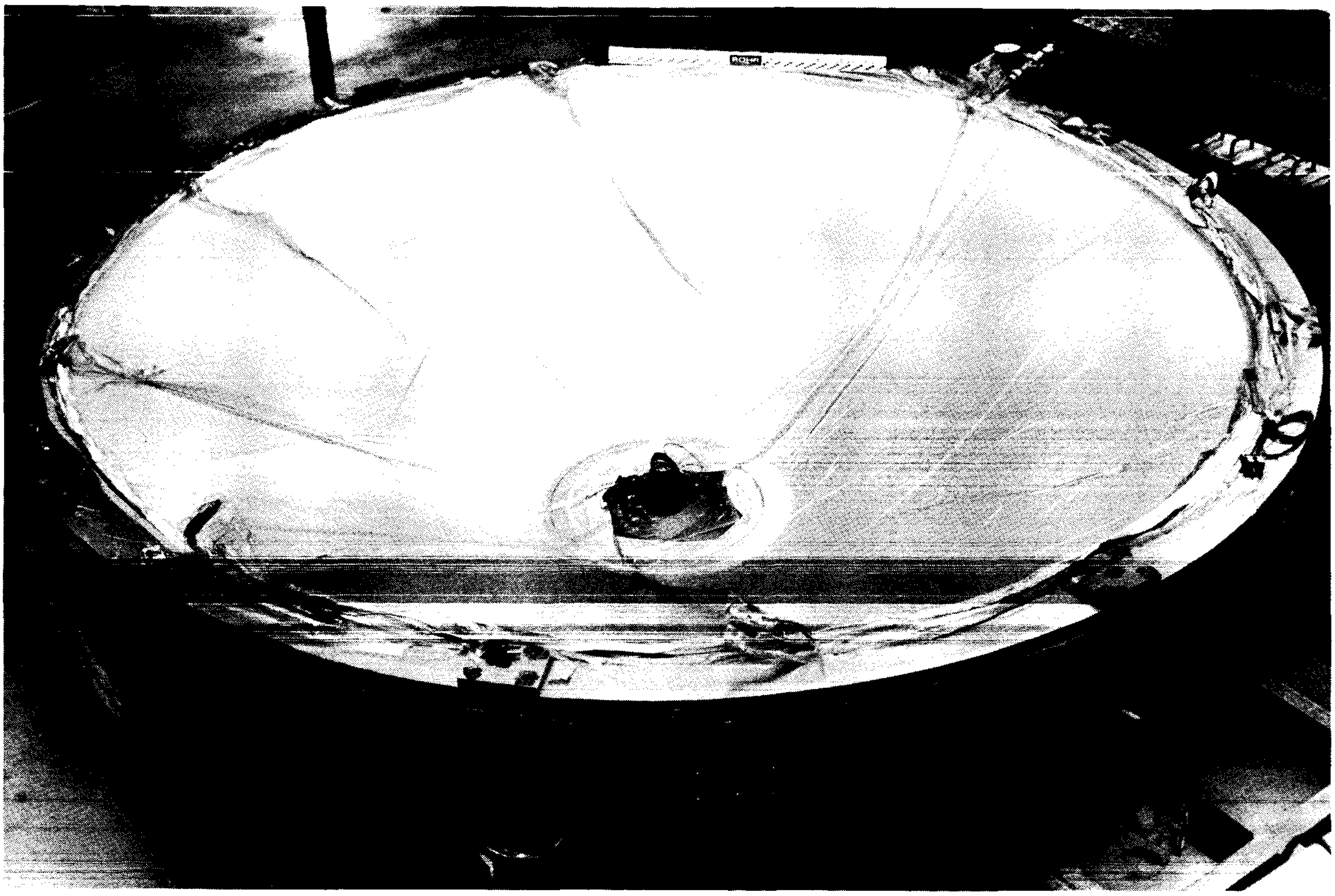

Fig. 26. Vacuum-bag setup

rotated 45 deg clockwise from the ply before. Vacuum bagging should be done with a formed bag so that there are no bag wrinkles in the area where the major cone mates to the aft cone. The finished aft cone may then be used as a pressure tool so that any bumps or discontinuities in the aft cone faying surface due to the original cure can be transferred in mirror image to the major cone. The vacuum-bag setup was that shown in Fig. 26. The bagging layup includes one layer of pink glass-release cloth, two layers of standard 181 glass cloth, and the nylon bag (see cross section in Fig. 27). Other bagging layups were tried, but provided less control of skin wrinkling. A tubing around the entire periphery of the bagging area ensured reasonably uniform application of the vacuum source. The difficult joint between the two bond jigs was sealed on the outer side by dropping a cord in the groove between the facesheet extension at the outer edge of the major cone and the aft cone bond jig surface, then bagging over the cord (Fig. 28). A pressure plate is also helpful at the forward ring to ensure a flat surface and eliminate bridging at the angle. A vacuum-bag cure, for ½ h at 300°F and 2 h at 350°F, is again used. After cure the 6-ply second skin has a dry texture and is slightly dimpled (Fig. 29) but less so than the 4-ply skin on the aft cone. The completed major cone (Fig. 30) may now be inspected.

D. Mating the Major and Aft Cones

With the two cones complete, the cones and their tools are assembled. Feeler gages are inserted in the gap between the two cones (Fig. 31) to determine the amount of adhesive necessary to provide a good joint. The aft cone and bond jig are removed from the major bond jig and the appropriate layers of supported epoxy adhesive are laid up on the faying surface of the main cone. The jigs and cones are then reassembled. Epoxy-foam potting compound is applied to the mating groove between cones (Fig. 32) and trowelled to contour per the drawing (Fig. 6). Adhesive is applied on the faying surface

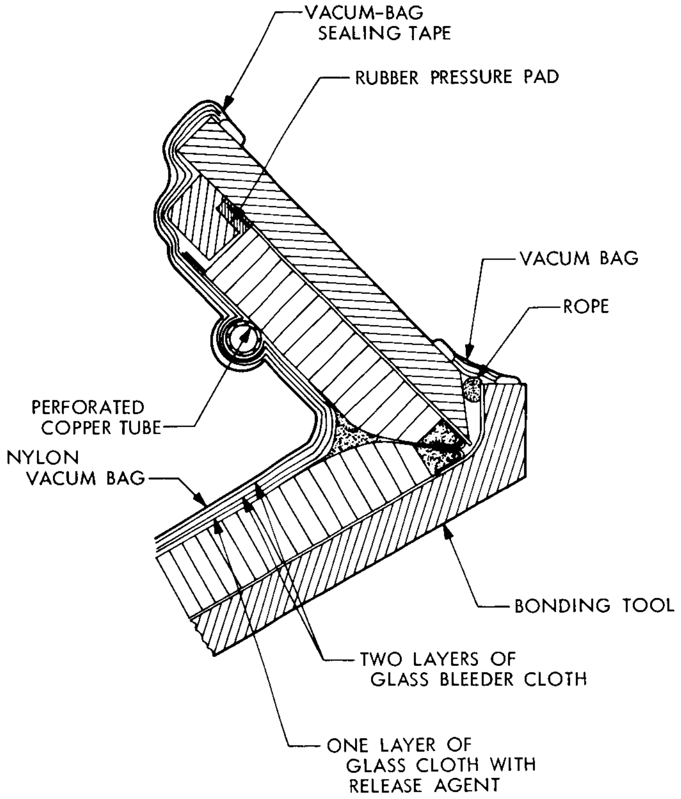
VACUM-BAG SEALING TAPE
RUBBER PRESSURE PAD
VACUM BAG
ROPE
PERFORATED COPPER TUBE
NYLON VACUM BAG
BONDING TOOL
TWO LAYERS OF GLASS BLEEDER CLOTH
ONE LAYER OF GLASS CLOTH WITH RELEASE AGENT

Fig. 27. Cross section of vacuum-bag layup

Fig. 28. Sealing joint between two bond jigs for vacuum-bagging

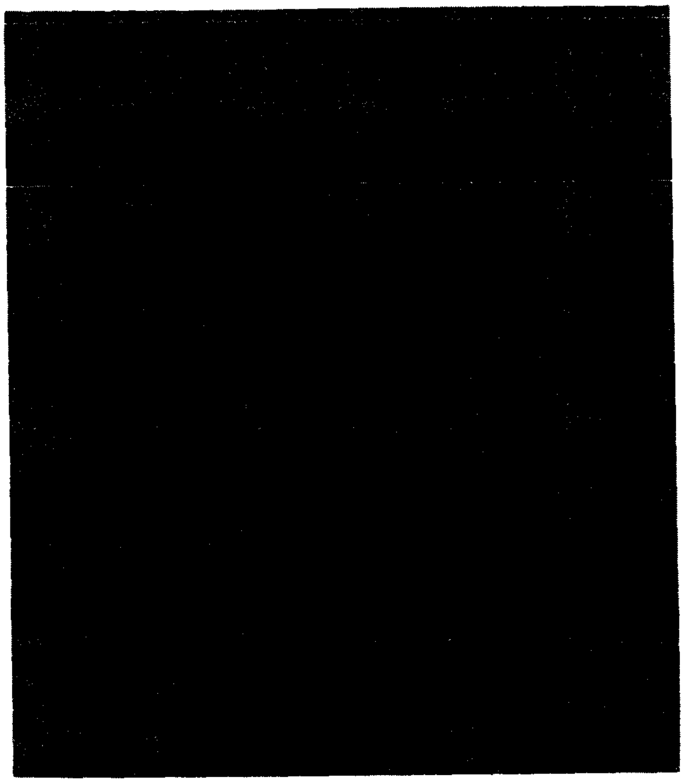

Fig. 29. Texture of inner skin on major cone

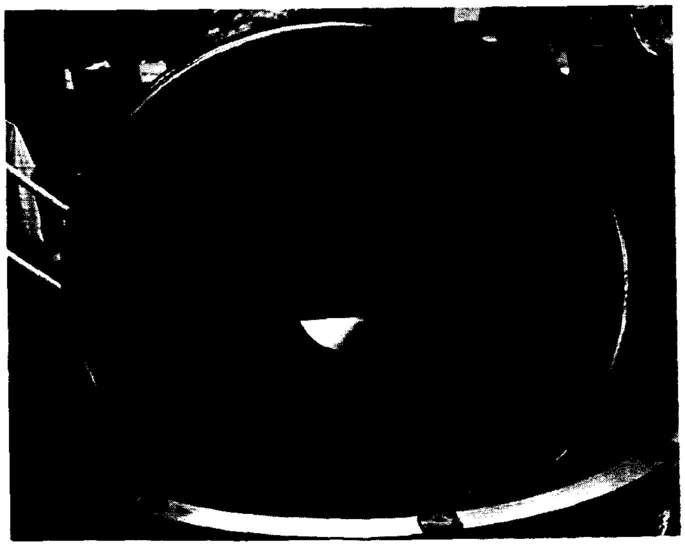

Fig. 30. Completed major cone

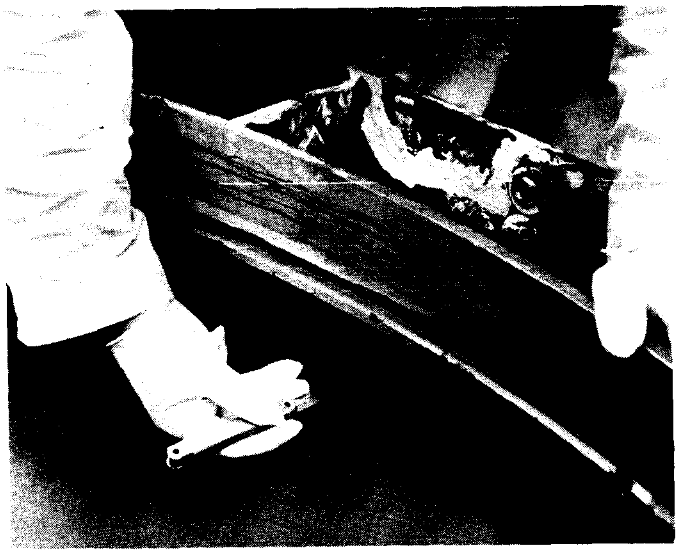

Fig. 31. Placing feeler gages between two cones to determine adhesive requirements at joint

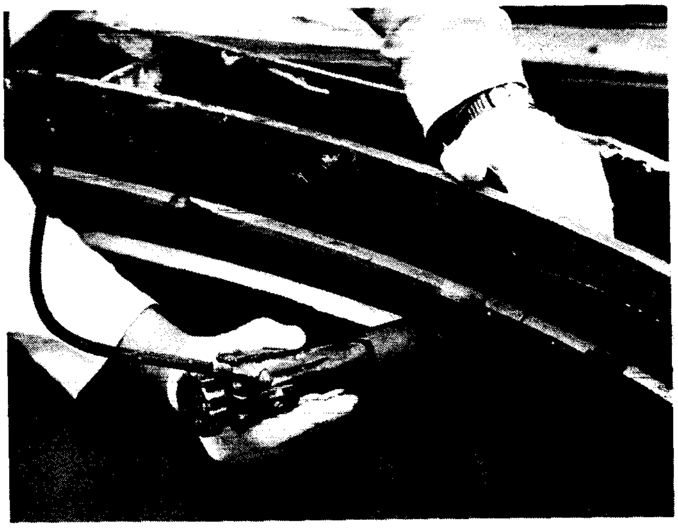

Fig. 32. Potting compound being gunned into mating groove

between the cones and the C-ring. The C-rings are fitted into place (Fig. 33) and are butted together tightly with inch-overlap, precured internal doublers cut back to the tangency point. The assembly is then vacuum-bagged and cured for 1 h at 350°F. After cure, the joint should be smooth and without distortion.

E. Finishing and Mating the Attachment Ring

The predrilled attachment ring skin is laid in the center bond tool with the holes positioned with threaded insert pins. Thirty-two inserts, with washers of the standard adhesive applied to the faying surface between the insert and the skin, are screwed in place, to be tight against the skin, and are aligned with the flattened edges

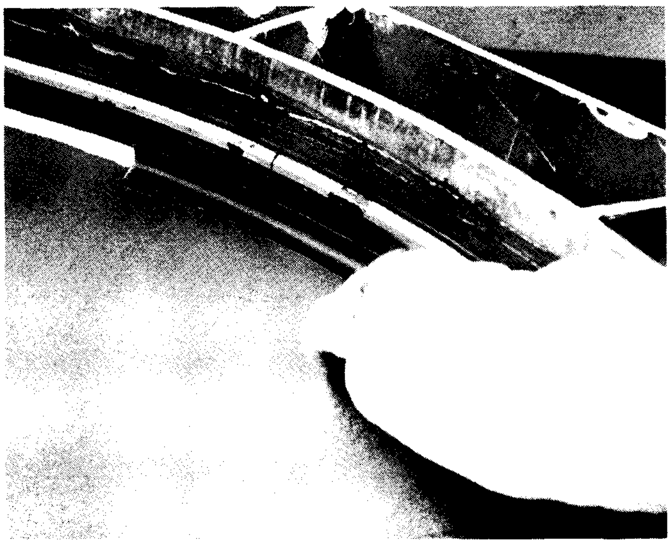

Fig. 33. Fitting C-rings in place

of the inserts circumferential (Fig. 34). The inserts are cured in place 1 h at 350°F to prevent insert misalignment and flow through the insert holes during application and cure of the potting compound. The epoxy foam potting compound is then applied to the attachment ring and trowelled to a reasonable flatness (Fig. 35). One ply of supported epoxy adhesive is applied to the faying surface of the main cone (Fig. 36). The center bond tool with attachment ring in place is then lowered onto the main conical surface, and cured for 1 h at 350°F under pressure. Upon disassembly, release of the attachment ring from the center bond tool is checked before proceeding. The entire aeroshell entering the oven for this final cure is shown in Fig. 37. After cure, the part is released from the tool and visually inspected before the final finishing operations are started.

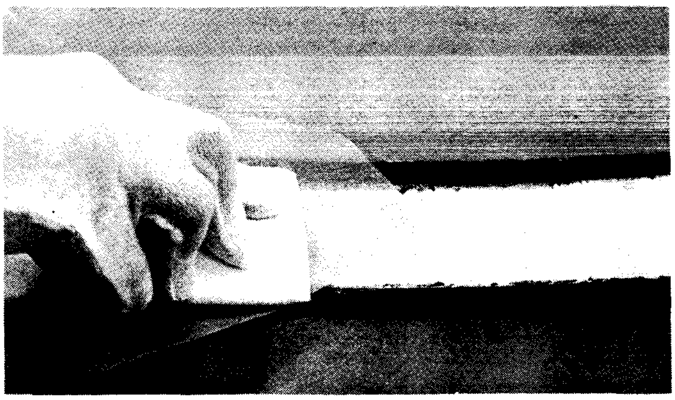

Fig. 35. Attachment ring with potting compound being troweled in place over inserts

F. Routing and Drilling the Forward Ring

The part is placed in the major bond jig for routing. A special routing tool is centered through the centerline

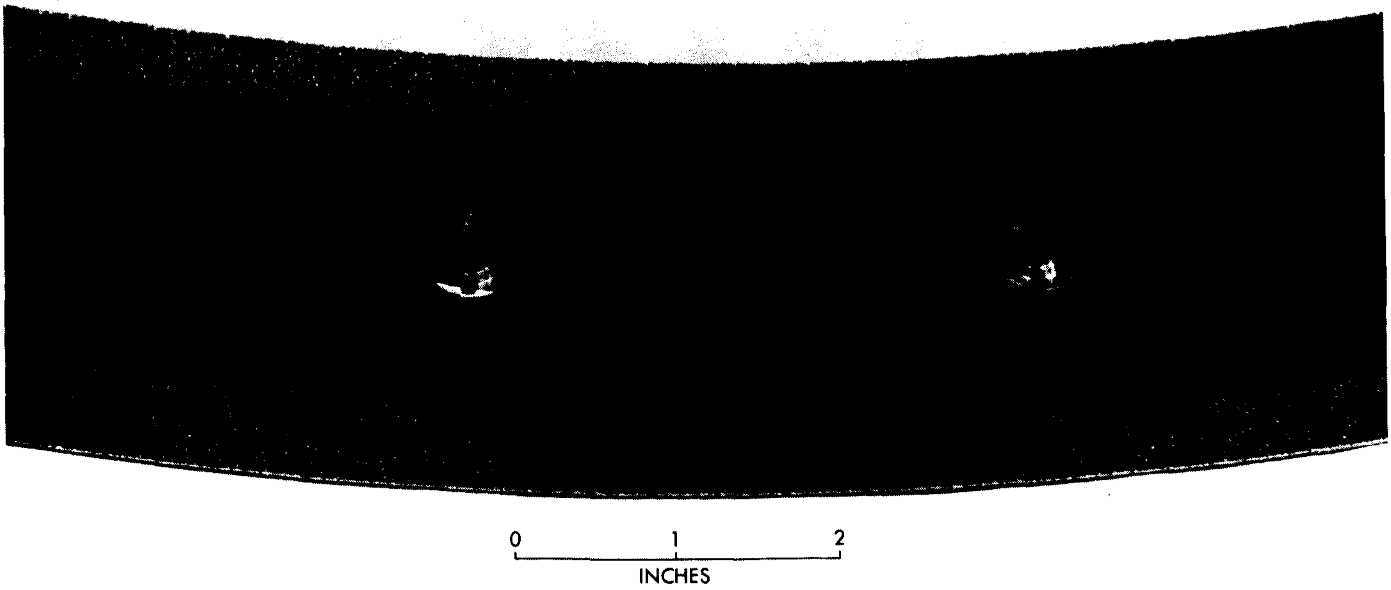

Fig. 34. Inserts in place in attachment rings

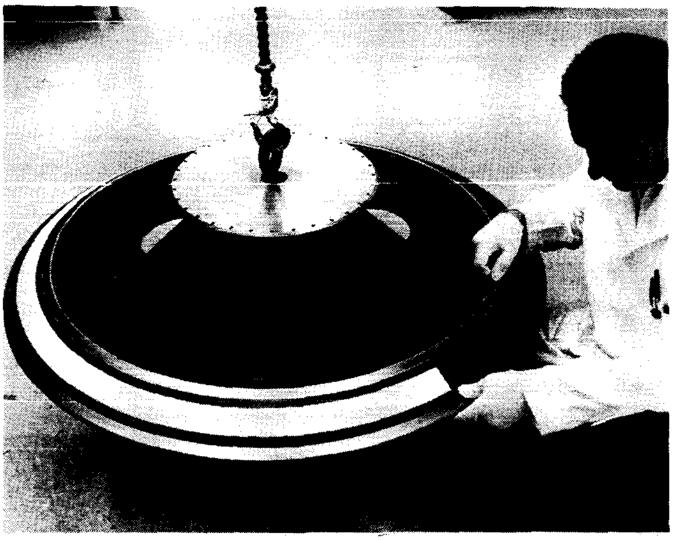

Fig. 36. Applying adhesive over potted attachment ring

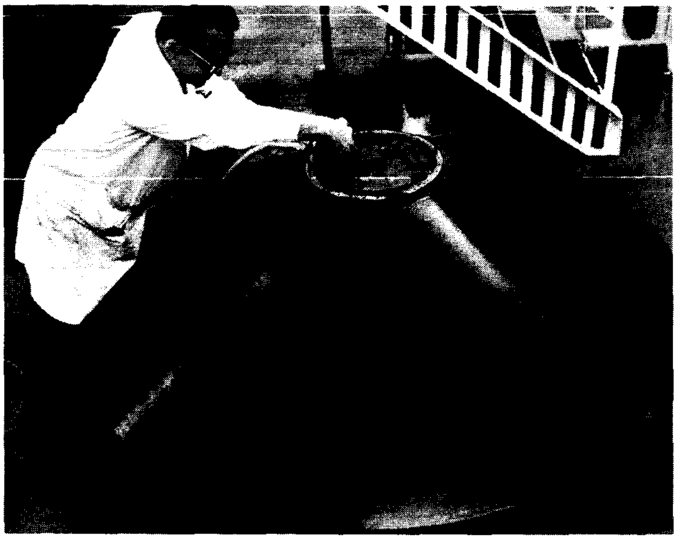

Fig. 38. Drilling holes at forward ring

Fig. 37. Aeroshell entering oven for final cure

bushing and turned by hand during the routing operation. Tolerance requirements for this surface were not sufficiently tight to warrant a more elaborate routing fixture. The holes in the forward ring were originally located and drilled with a plate attached on the center bond tool. Under this situation, the need to use a hand drill inside the center bond tool provided sloppy location and elongated holes. For the second aeroshell a drill bushing plate was made, keyed to the first locating plate, to allow drilling from outside the center bond tool (Fig. 38). The finished aeroshell structure, which weighed 37.7 lb, is shown in Figs. 39 and 40.

IV. Inspection of Basic Conical Structure

Inspection at any point in the entire fabrication procedure is primarily visual. Obvious bond imperfections or poor workmanship were repaired or redone. The bond between the facesheets and the core was inspected by coin tapping (Fig. 41). Other nondestructive test methods were felt to be unsuitable, either because of unacceptable contamination from necessary contact liquid or because of expense or availability. Using the crude coin tapping technique, it was found that unbonded areas down to a size of ½ in. in diameter could be readily identified on flat samples from which adhesive had purposely been omitted. No unbonded areas were discovered during normal fabrication procedures.

Rough dimensional tolerances were inspected on a large Niles lathe using dial indicators (Fig. 42). The 39-in. bolt circle on the major attachment ring was within 2 mils of the centerline of the cone and varied only 5 mils out of round. The forward bolt circle at the 15.5-in. diameter was within 8 mils of true position with the attachment ring bolt circle. The attachment ring bolt circle surface was flat to within 10 mils. Spinning the cone to determine out of round tolerances for ablator application provides the polar chart shown in Fig. 43. Variation appears to be within the 30 mils specified in Fig. 6. Distortions are partly due to small, but apparent, local buckling and partly due to slop in the lathe turning operation.

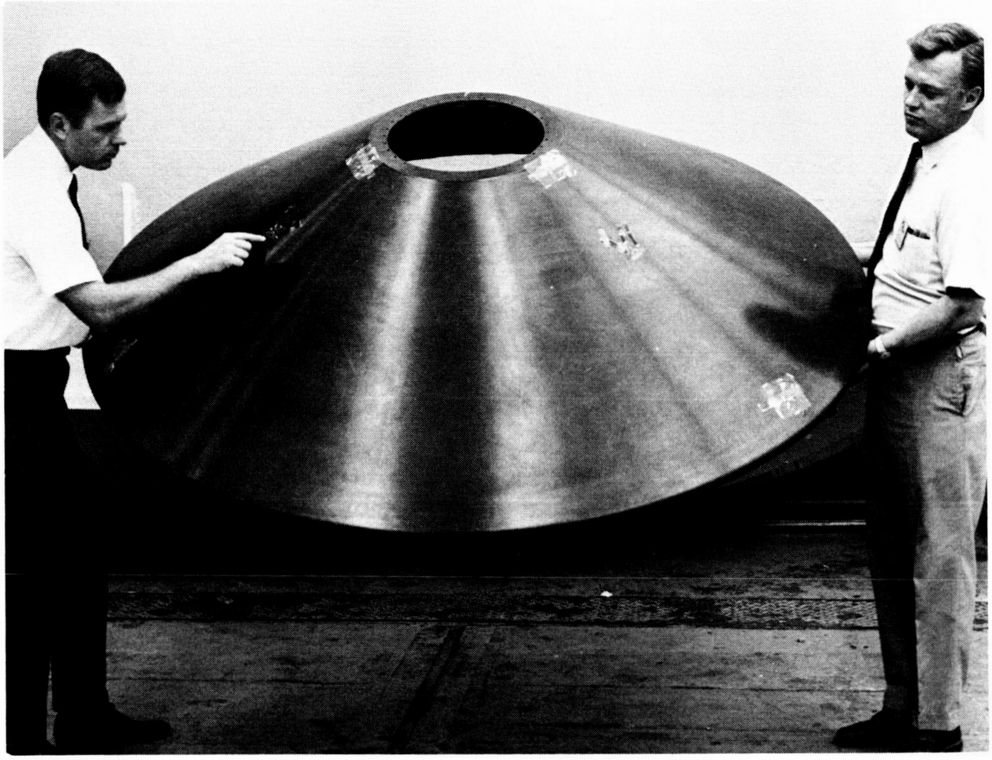

Fig. 39. Front view of finished structure

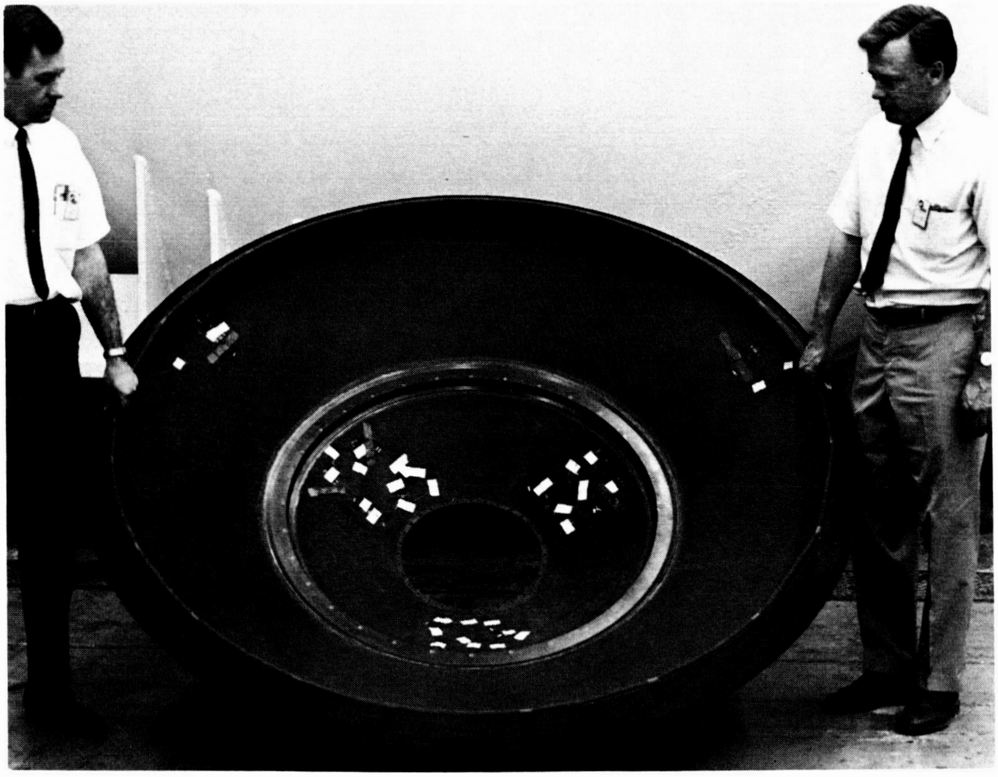

Fig. 40. Rear view of finished structure

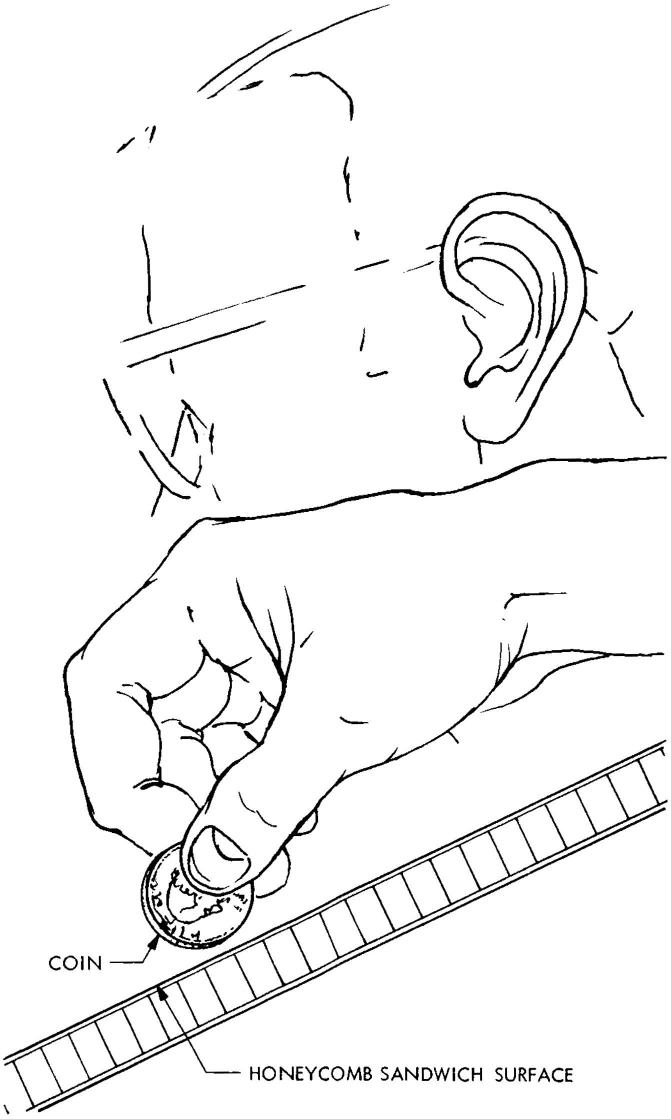
COIN
HONEYCOMB SANDWICH SURFACE

Fig. 41. Inspecting core-to-facesheet bond

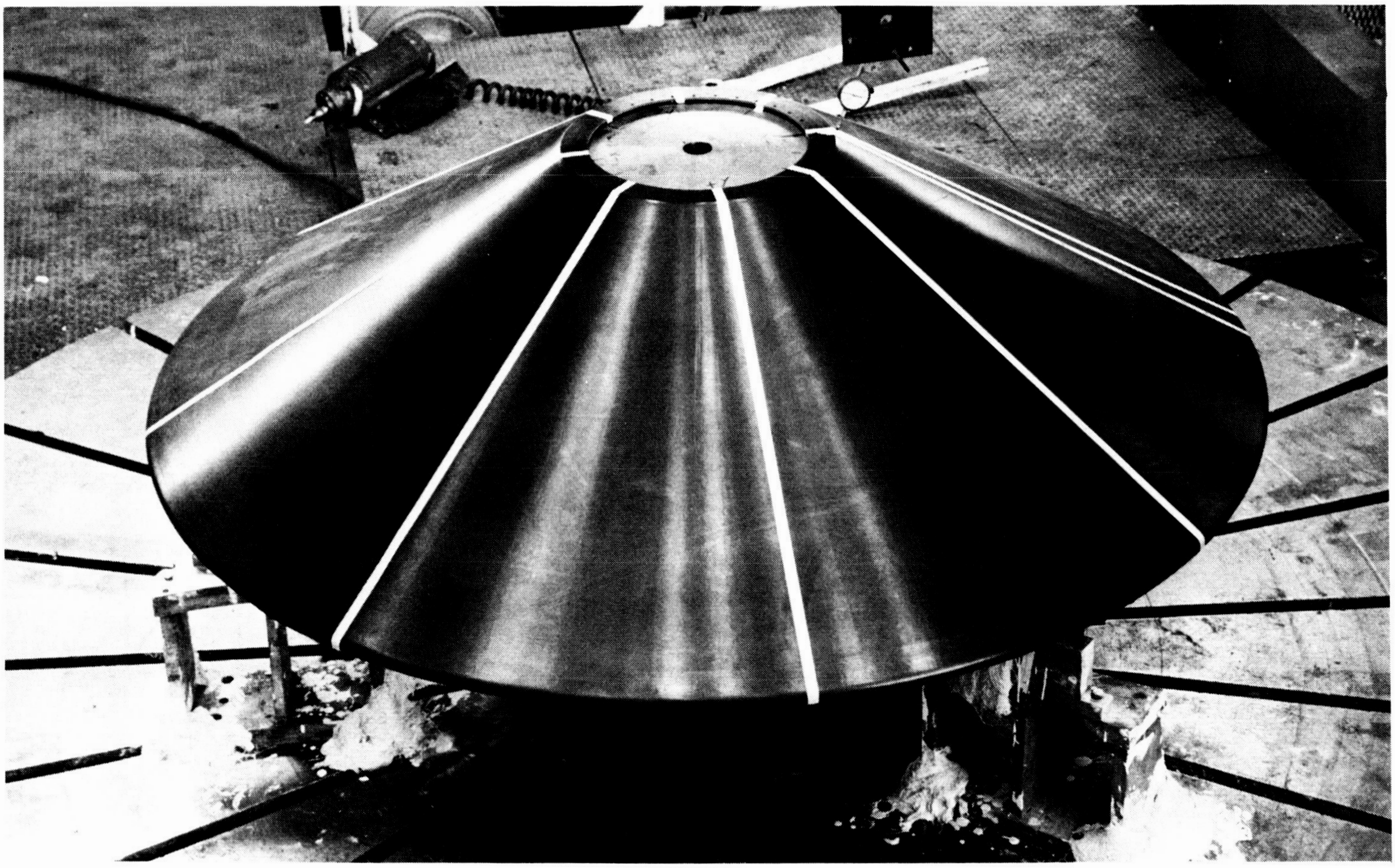

Fig. 42. Out-of-round inspection setup at Rohr

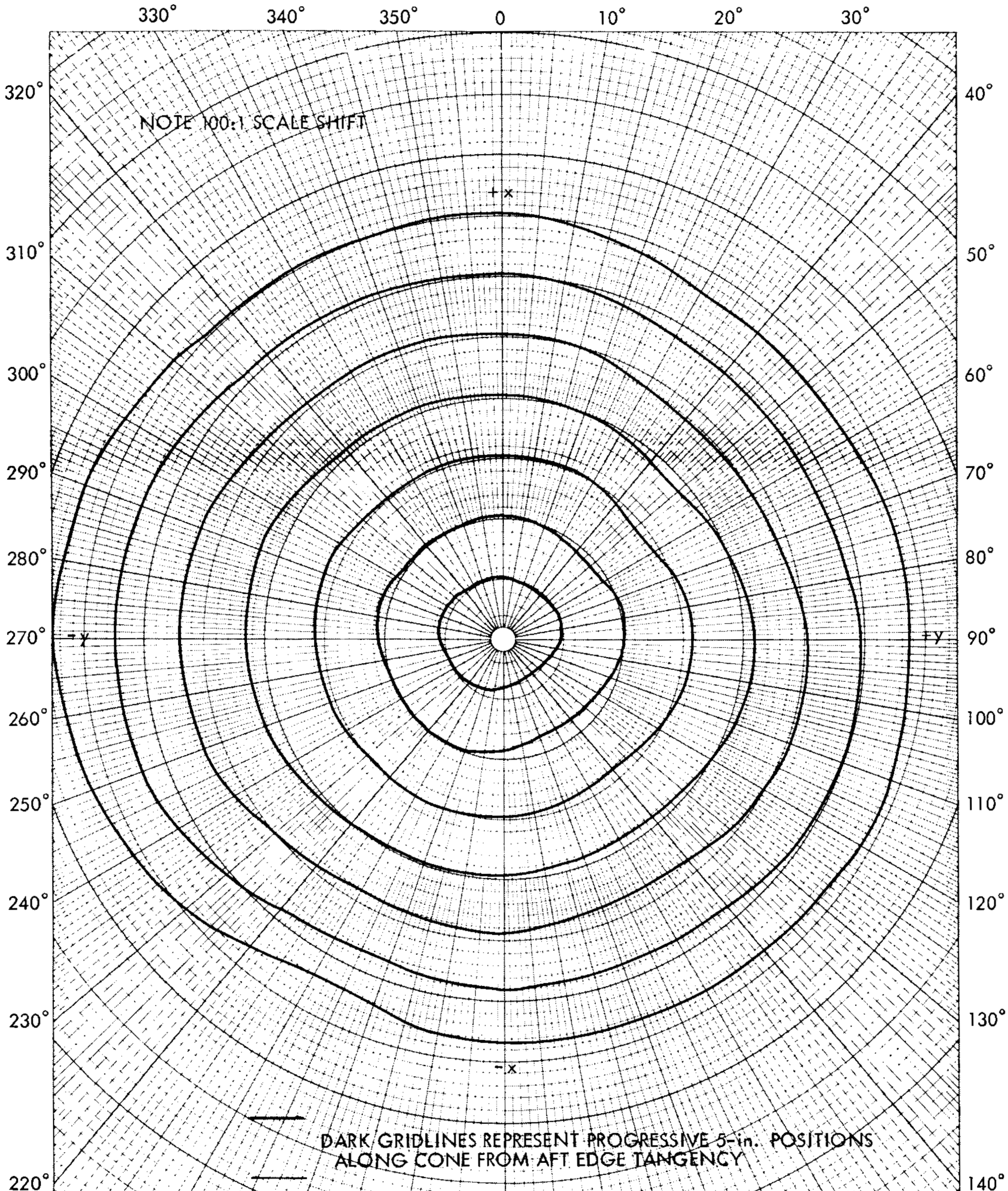

Fig. 43. Polar chart of out-of-round measurements on structure

V. Nosecap and Ablator

A. Steel Dome

The 405 stainless steel dome was machined from 4-in.-thick plate to the configuration shown in Fig. 7. The finished dome is shown in Fig. 44. The dome, fitted in place without heat shield, is shown in Fig. 45.

B. Ablator Application and Machining

The aeroshell structure, without the metallic dome, is placed on the coating fixture (Fig. 46). The teflon gasket and fiberglass insulator are positioned in place, and the insulator is pinned to the shell to prevent lateral movement. The ablator is applied in a semifluid state by rollercoating the material on the cone in the same fashion that one might paint a house (Fig. 47). The ablator is then vacuum-bagged (Fig. 48) and cured; the process produces the thick, nonfriable buildup shown in Fig. 49. The ablator is then mounted on a separate machining fixture made from fiberglass and aluminum tubing and is mounted on a large tape-controlled Bullard lathe (also shown in Fig. 49). The mating surface for the dome at the forward end is machined first, with care taken to center on the same line as the cone and to fair in smoothly with the insulator. A closeup of this surface and the key-like ridge matching the circumferential groove in the mating dome surface is shown in Fig. 50. The cone is then machined circumferentially under tape control to produce the taper shown in Fig. 6. The filled silicone elastomer material machines easily and provides the smooth conical surface shown in Fig. 51.

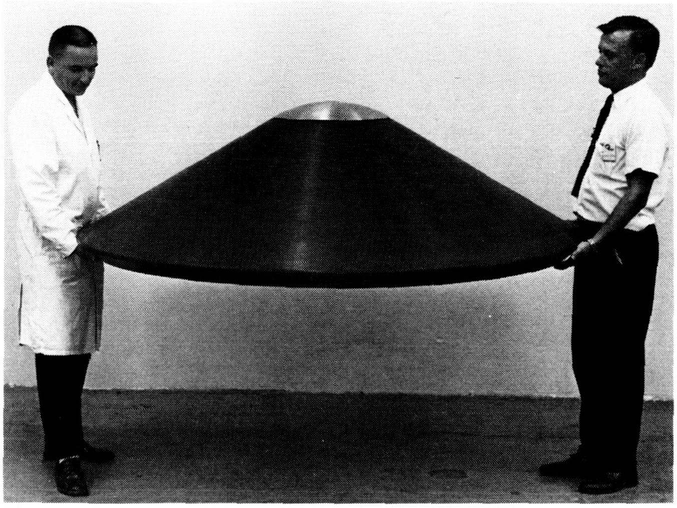

Fig. 45. Dome in place on structure

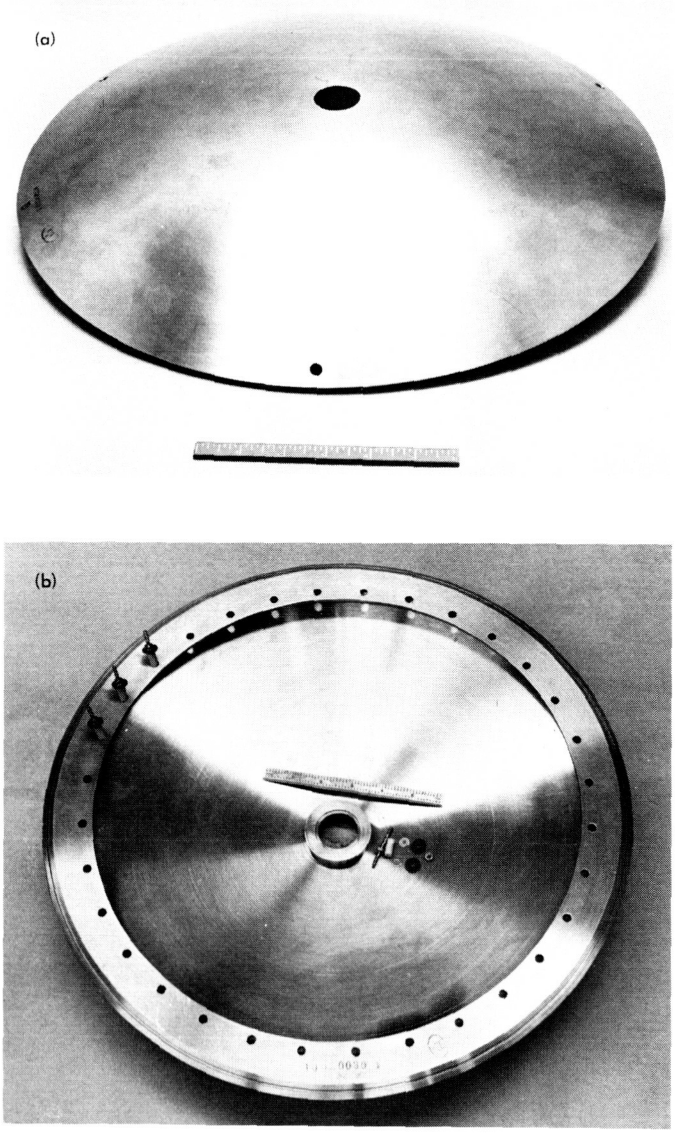

Fig. 44. Spherical metallic dome

VI. Final Inspection of Completed Aeroshell

The completed aeroshell, with the dome in place, is shown in Fig. 52. Excess heat shielding is found by weighing the aeroshell. (In the subject case, the aeroshell weighed 55 lb, which implied a 6-lb excess of heat shield material.) For final inspection the aeroshell is again spun on a lathe similar to that done earlier to determine the out-of-round of the final aerodynamic structure. Matching these measurements with the earlier polar charts shows similar concentricity. To check these measurements, the aeroshell is also inspected on a rotating table at JPL (Fig. 53). Local depth of the heat shield

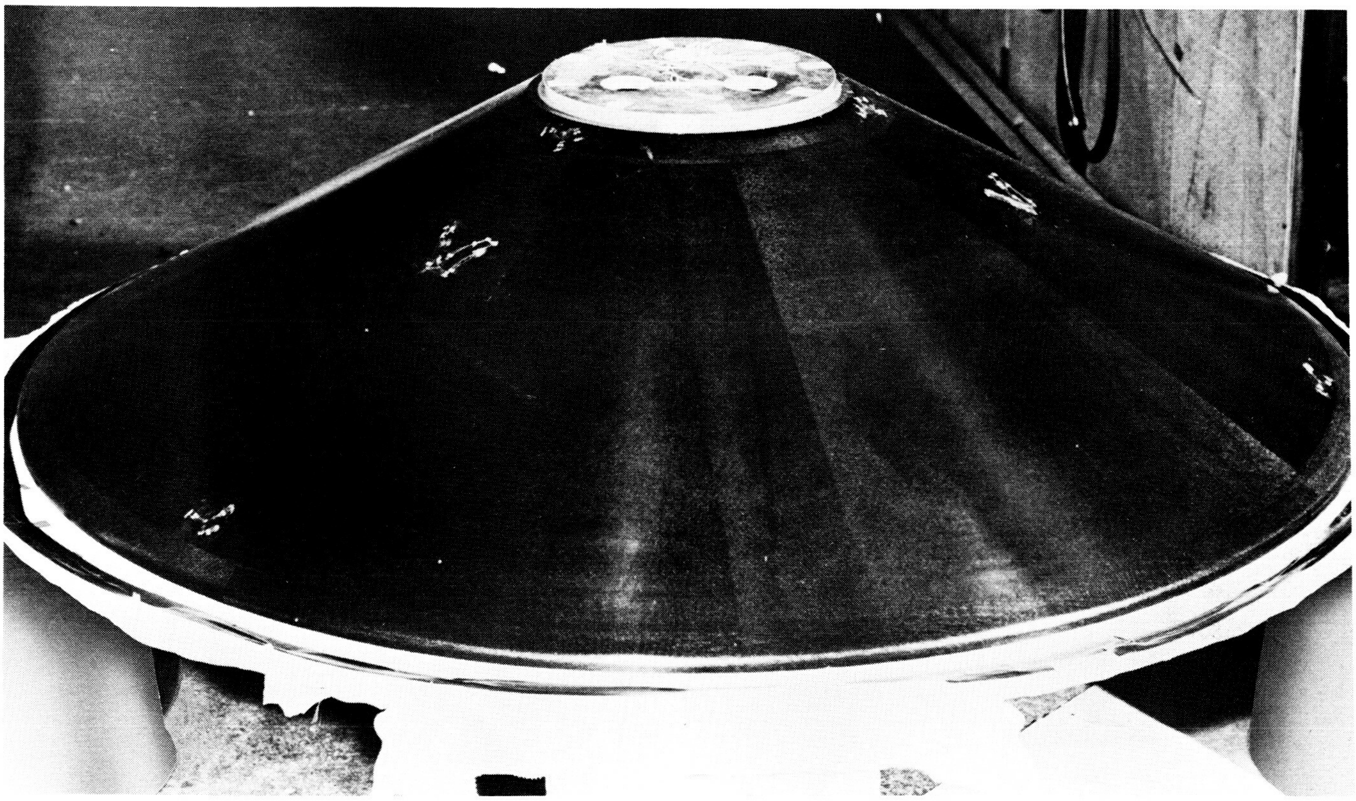

Fig. 46. Aeroshell structure mounted on coating fixture

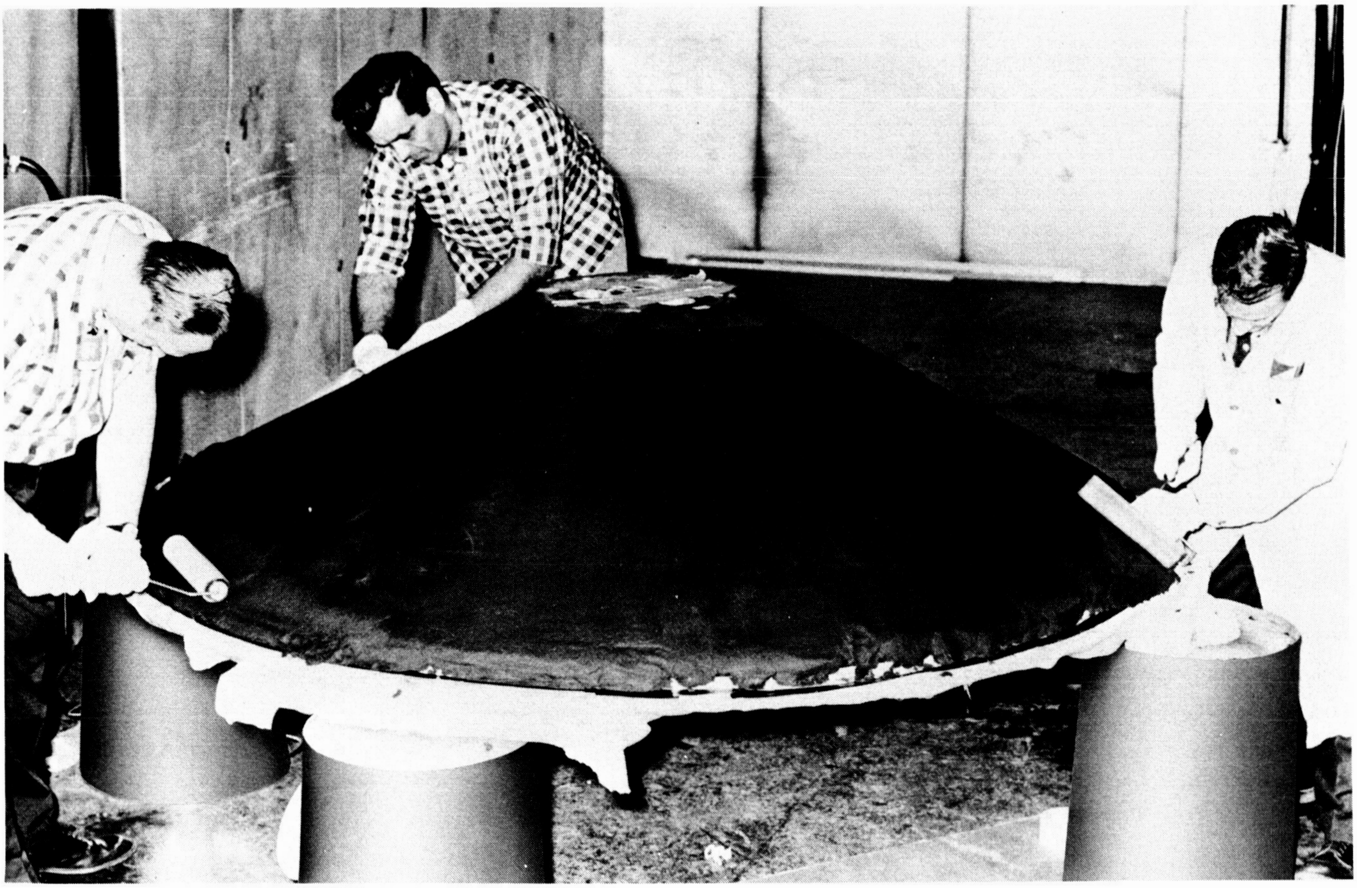

Fig. 47. Roller-coating ablator on major cone

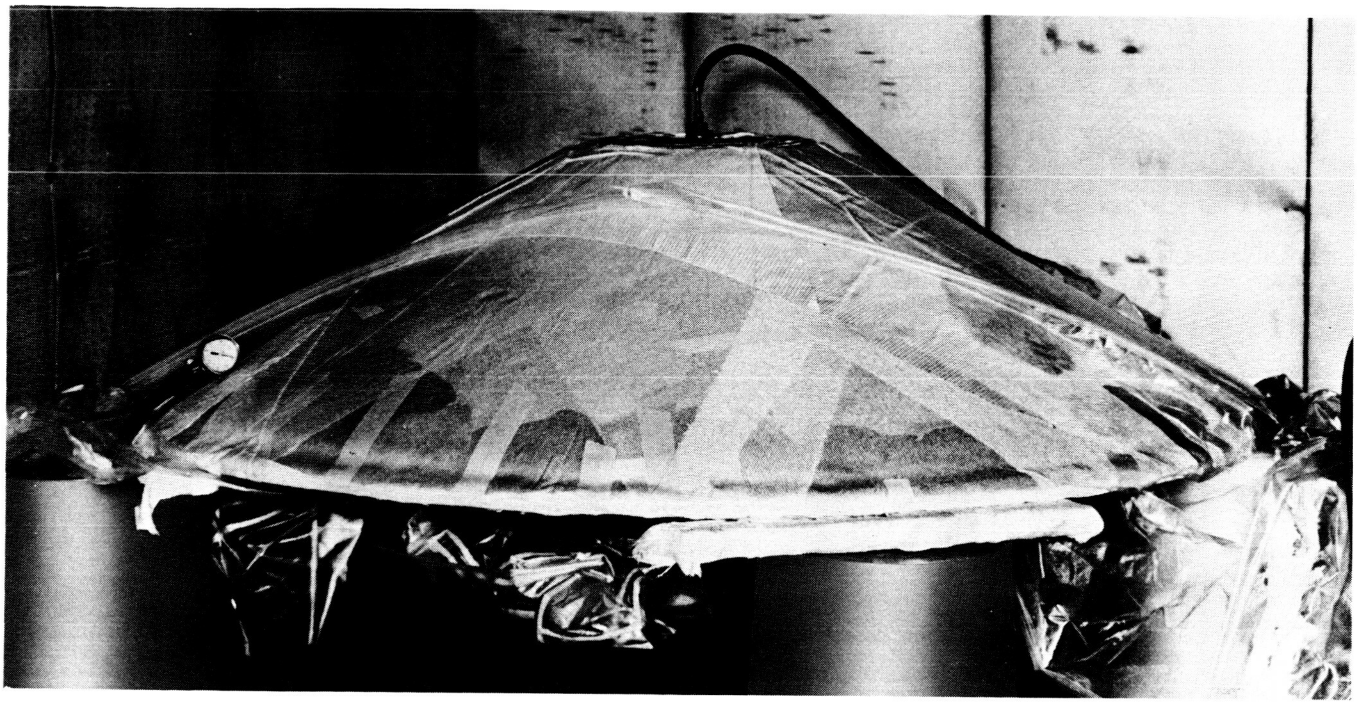

Fig. 48. The ablator vacuum-bagged

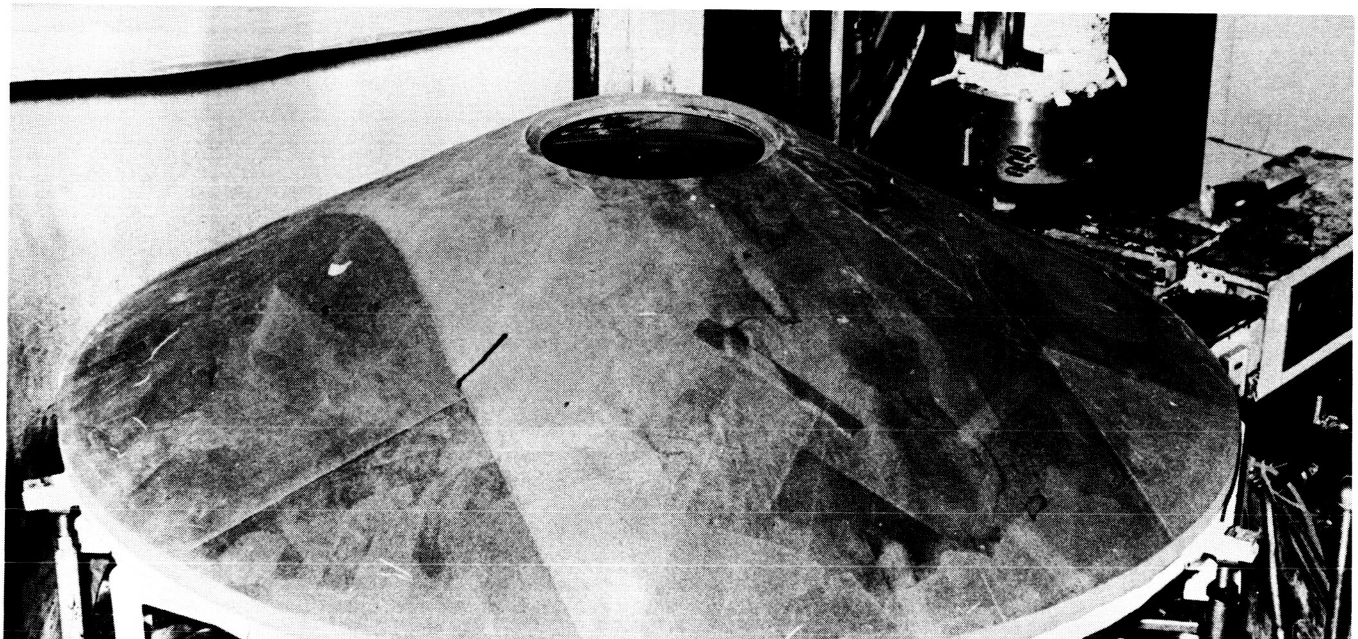

Fig. 49. Aeroshell with cured ablator mounted on machining fixture

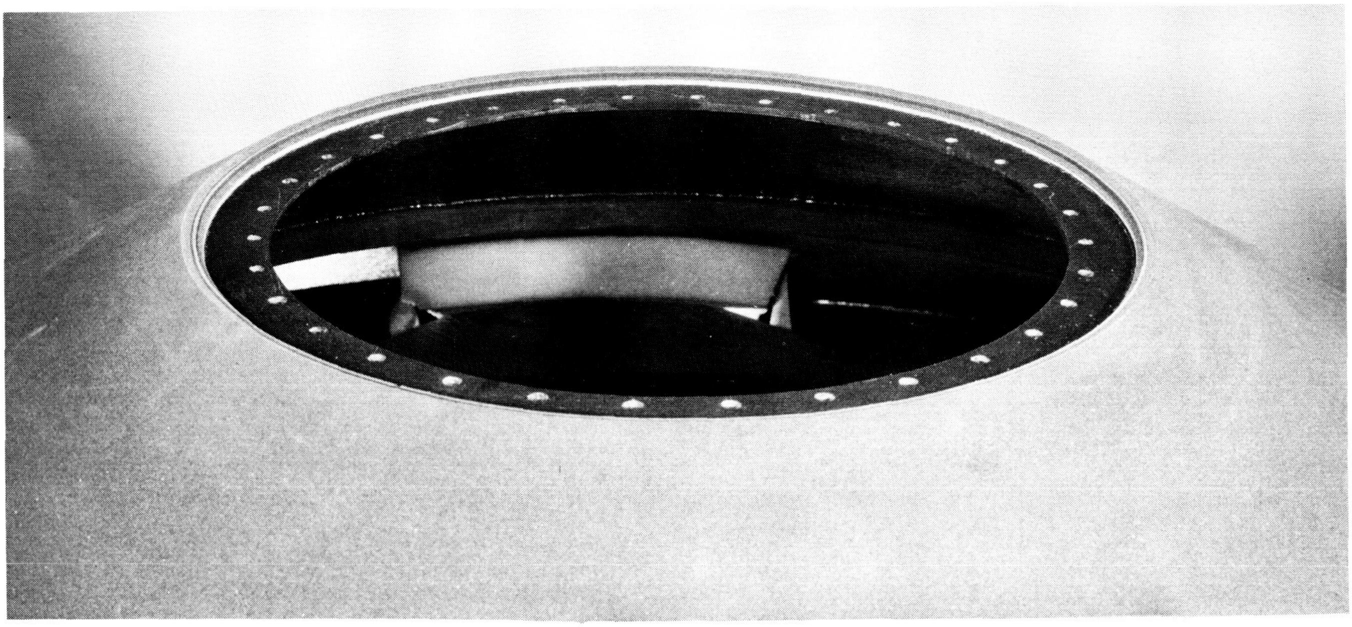

Fig. 50. Machined ablator surface at dome interface

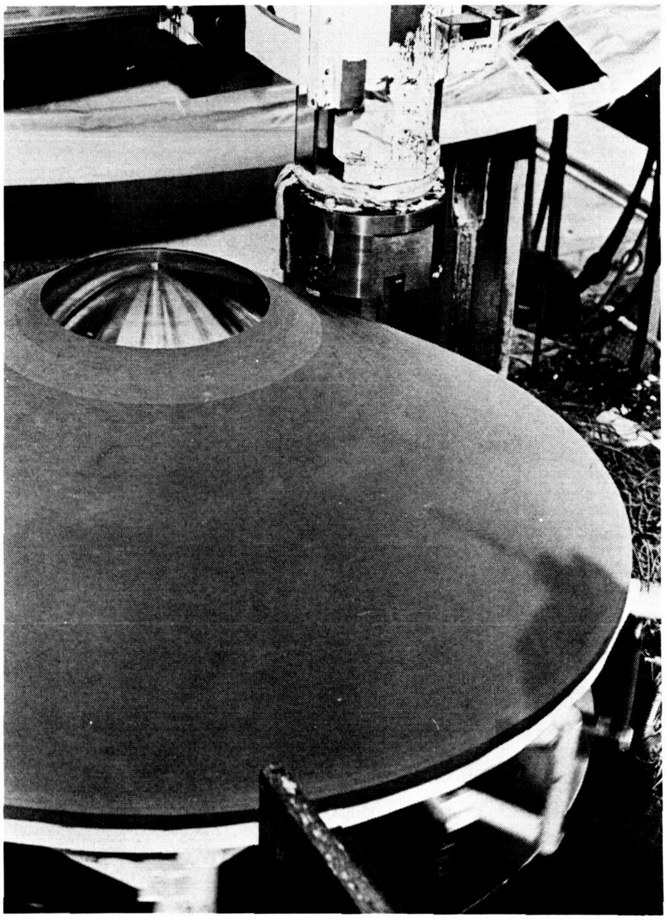

Fig. 51. Machined conical ablator surface

was measured (Fig. 54) with a dial indicator adapted for ablator penetration (Fig. 55). The dial indicator extension penetrates the ablator easily with less than 10 lb of force but stops at the fiberglass surface reproducibly to a mil. Table 3 shows the variation in ablator thickness over the cone. Figure 56 sums the final inspection of the aeroshell. On the average, surfaces were determined for the heat shield and structural interfaces. The on-the-average surface of the structural cone was within 0.05 deg of the design surface, which is considered excellent for a fiberglass structure. The ablator was left too thick because of lack of understanding in the initial inspection measurements. This excess in thickness and variations in ablator density account for much of the observed 6-lb excess in ablator weight.

VII. Repair Techniques

Repair for a phenolic fiberglass structure is reasonably easy. On the second aeroshell, bulging of the inner skin on the major cone at the outer curvature during cure necessitated removal and replacement of the entire inner skin. The skin peeled off without apparent damage to the core. The only loss in putting on the new skin was additional weight resulting from inability to remove all of the original adhesive.

If local areas on the cone are detached for such reasons as poor fabrication (not observed), tool release

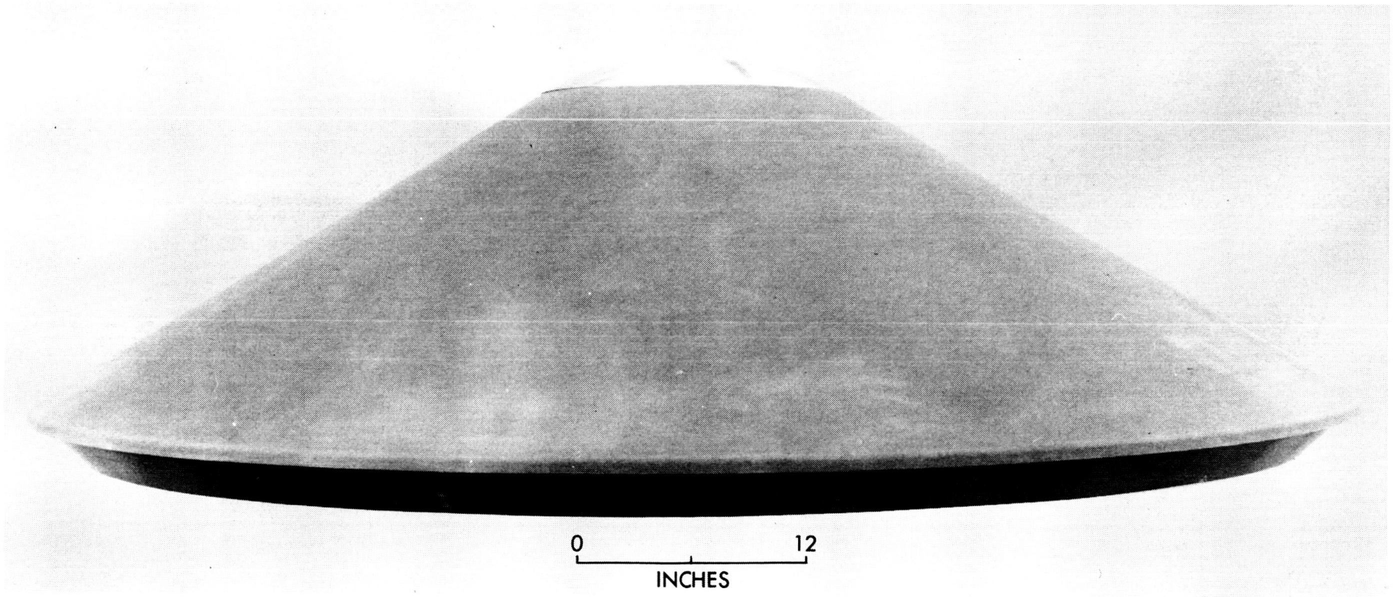

Fig. 52. The completed aeroshell

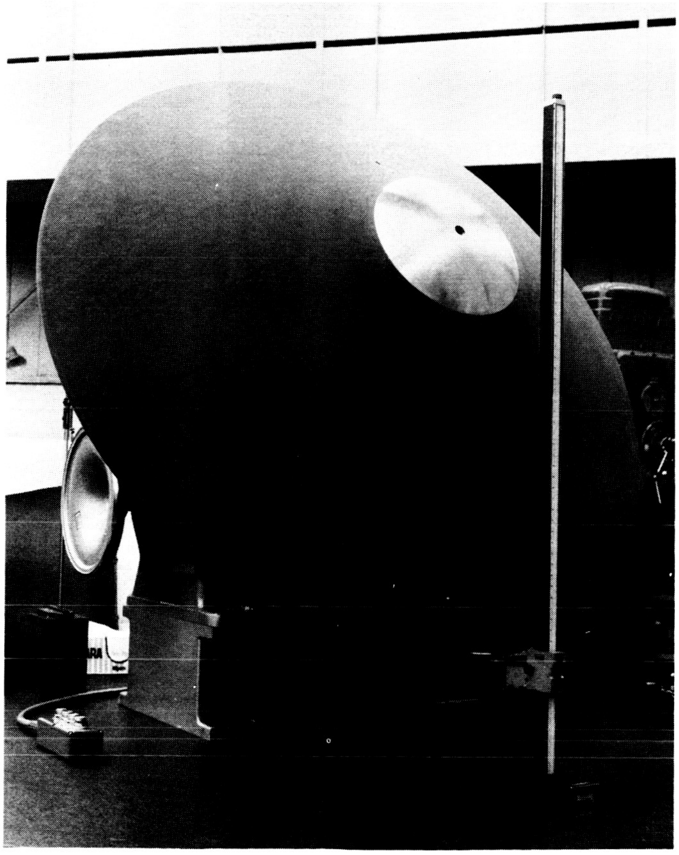

Fig. 53. Aeroshell on inspection fixture at JPL

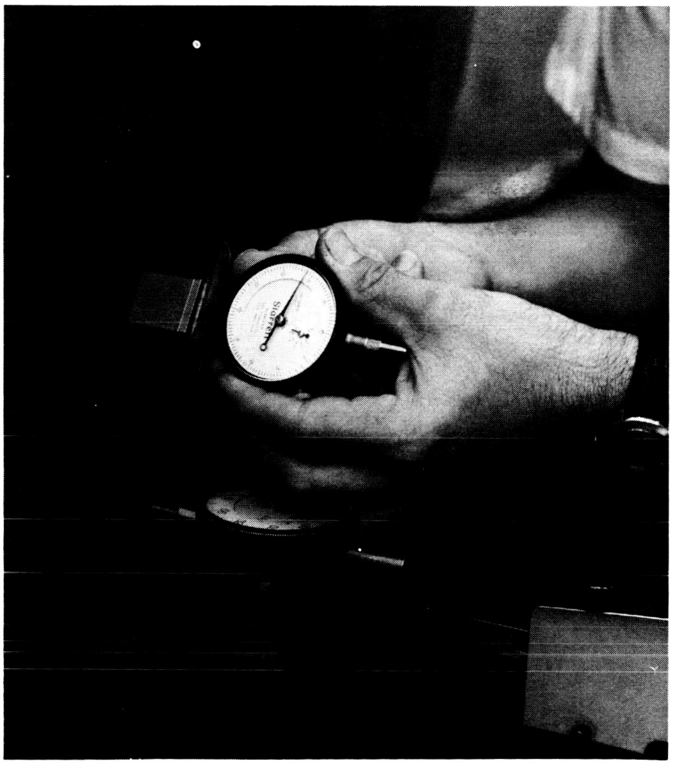

Fig. 54. Heat shield thickness-determination setup

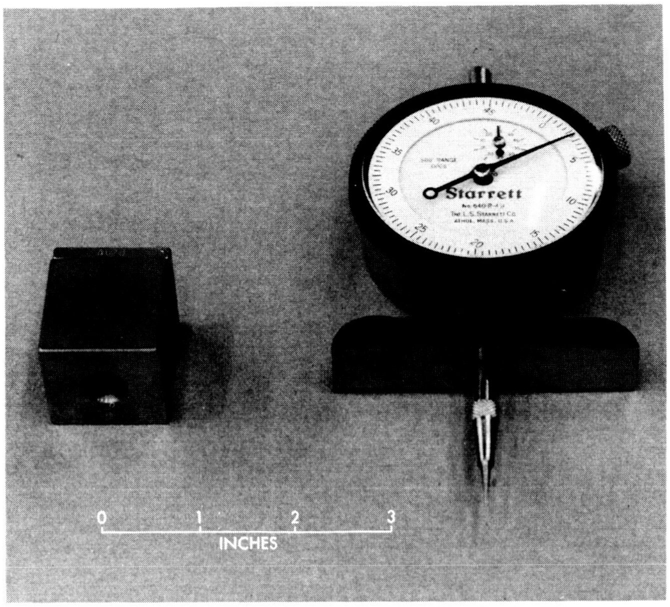
Starrett
0
1
2
3
INCHES

Fig. 55. Dial indicator with pointed tip

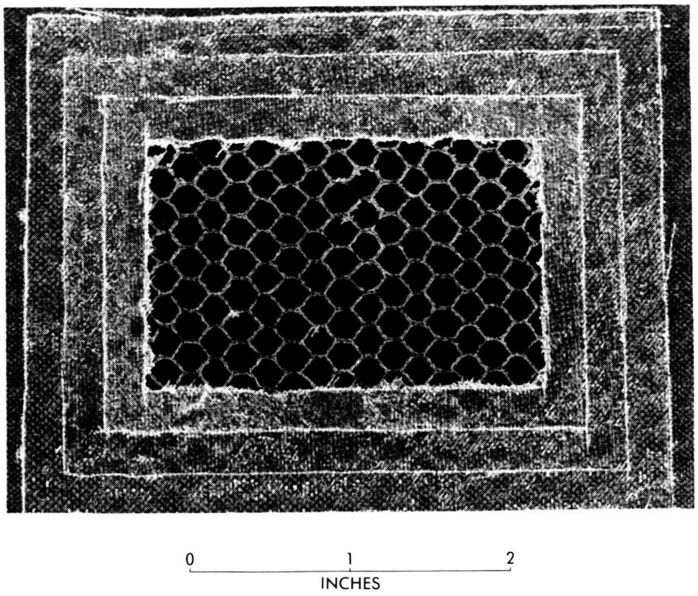

Fig. 57. Facesheet repair technique

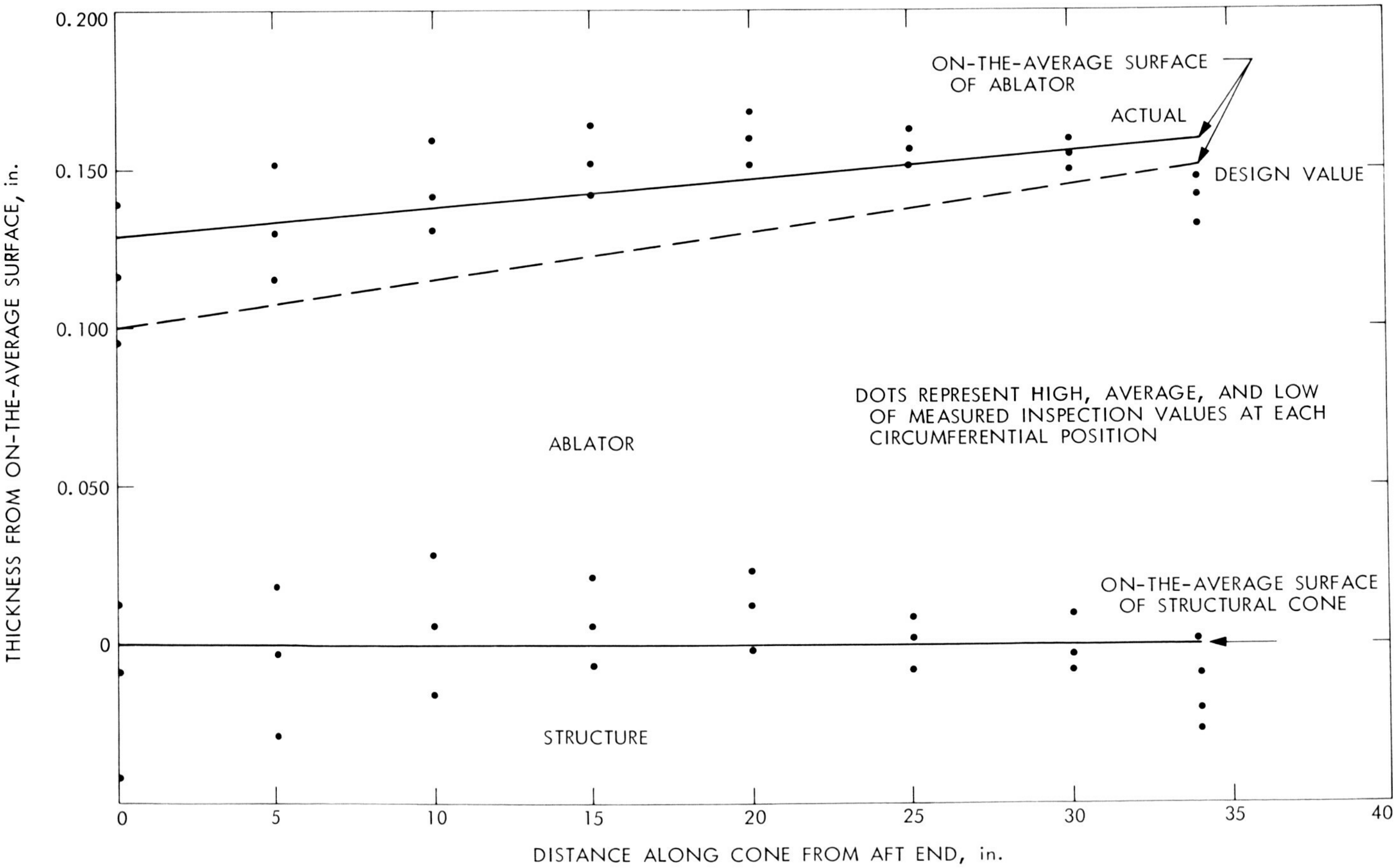

Fig. 56. Final inspection of aeroshell

problems (observed on the first shell before the attachment ring taper was added), or careless handling (the night shift punched a hole in the outer skin of the aeroshell with a dolly), repair was found to be reasonably straightforward. The skin could be locally removed with a razor, one ply at a time, with each outward ply removed back by ¼ in. farther than the ply below. A sample repair area in process is shown in Fig. 57. The new face may then be laid back, one ply at a time, and the resultant area has properties within 90% of the original properties. Several areas on the first cone were replaced in this manner.

Insufficient precautions during bagging the main cone — for cure of the core to the first facesheet — can cause local buckling of the core along the outer periphery. The buckled core may be cut out carefully and new core spliced in place with foam adhesive. Figure 58 shows the splice actually made in the second aeroshell. When the edge of the cone was routed to allow insertion

Table 3. Variation in ablator thickness along cone

Radial position along cone, in.	Local ablator thickness, in.															
	Angular variation around axis, deg															
	0 (+x)	22½	45	67½	90 (+y)	112½	135	157½	180 (−x)	202½	225	247½	270 (−y)	292½	315	337½
0.000	0.105	0.146	0.152	0.137	0.120	0.123	0.130	0.139	0.139	0.133	0.127	0.111	0.100	0.104	0.106	0.102
5.000	0.126	0.146	0.149	0.145	0.124	0.121	0.138	0.152	0.146	0.141	0.138	0.120	0.112	0.107	0.115	0.130
10.000	0.131	0.147	0.151	0.145	0.128	0.122	0.143	0.145	0.146	0.142	0.142	0.124	0.121	0.115	0.125	0.135
15.000	0.147	0.155	0.155	0.151	0.137	0.137	0.150	0.155	0.154	0.146	0.149	0.136	0.135	0.130	0.140	0.145
20.000	0.149	0.155	0.160	0.150	0.138	0.141	0.150	0.152	0.157	0.145	0.150	0.142	0.142	0.138	0.141	0.146
25.000	0.159	0.156	0.167	0.161	0.150	0.157	0.163	0.155	0.158	0.152	0.151	0.146	0.148	0.147	0.146	0.151
30.000	0.163	0.158	0.165	0.164	0.162	0.165	0.159	0.162	0.165	0.151	0.158	0.155	0.155	0.153	0.153	0.155
34.000	0.167	0.162	0.161	0.162	0.158	0.160	0.162	0.162	0.169	0.156	0.157	0.158	0.158	0.156	0.160	0.163

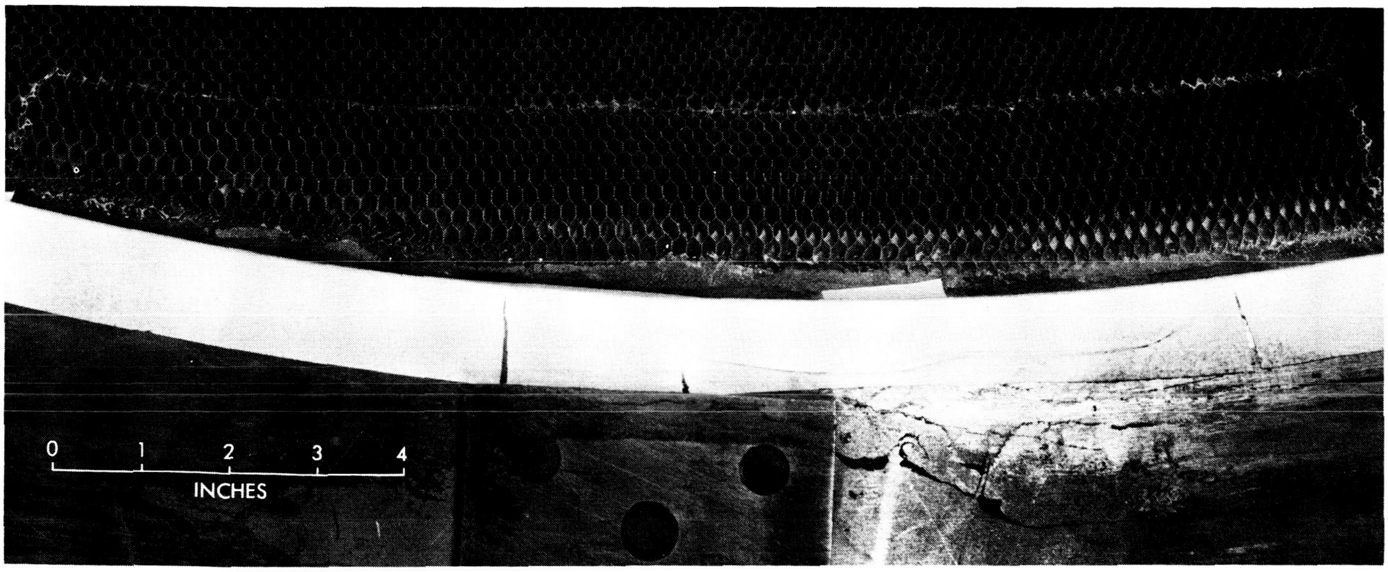

Fig. 58. Core repair area

of the V-ring, this splice was reduced to about 1 to 2 in. wide and about 15 in. long.

Other kinds of repairs are much less desirable, although in the first aeroshell a 3-in. piece was replaced on the attachment ring because of inadvertent damage. The new piece was spliced in smoothly without apparent change in composite strength, but the repaired part was not able to meet the flatness tolerances established for that ring, and local distortions made release from the tools more difficult.

VIII. Supplementary Studies and Tests

Some of the work reported earlier, as part of the advanced development program, is expanded here because of its particular reference to the specific mission in mind at the time this aeroshell was designed.

A. Sterilization

Samples of the honeycomb sandwich material were exposed to ethylene oxide (ETO) gas for surface decontamination (a total of 168 h at 50°C, etc.) and dry heat sterilization [a total of 552 h at 135°C, etc. (Ref. 3)]. The appearance of the samples was unaltered, except for a quite noticeable deepening of the red shade in the resin. Even in black and white, this shows as a darkening (see lower sample in Fig. 59). The mechanical properties of the composite sandwich improved by 10 to 25%. Most of this can probably be attributed to a post-curing effect.

B. Vacuum Testing

Samples of the honeycomb sandwich material were tested for thermal-vacuum stability, using the Micro-VCM test method developed for JPL by Stanford Research Institute (Ref. 4). Typical results and a description of the test apparatus and procedure are given in Ref. 5. The sample was vacuum-bag cured for ½ h at 300°F, followed by 2 h at 350°F. The weight loss was 0.7%, and the VCM (volatile condensable material) was 0.01%. The criteria used at JPL for selecting polymeric materials for general spacecraft use are 1.0% maximum weight loss and 0.1% maximum VCM. These results for the test samples are conservative, because parts of the actual aeroshell receive up to seven cure cycles during fabrication.

Mechanical properties in a vacuum were also felt to be important. The available data are confusing in that,

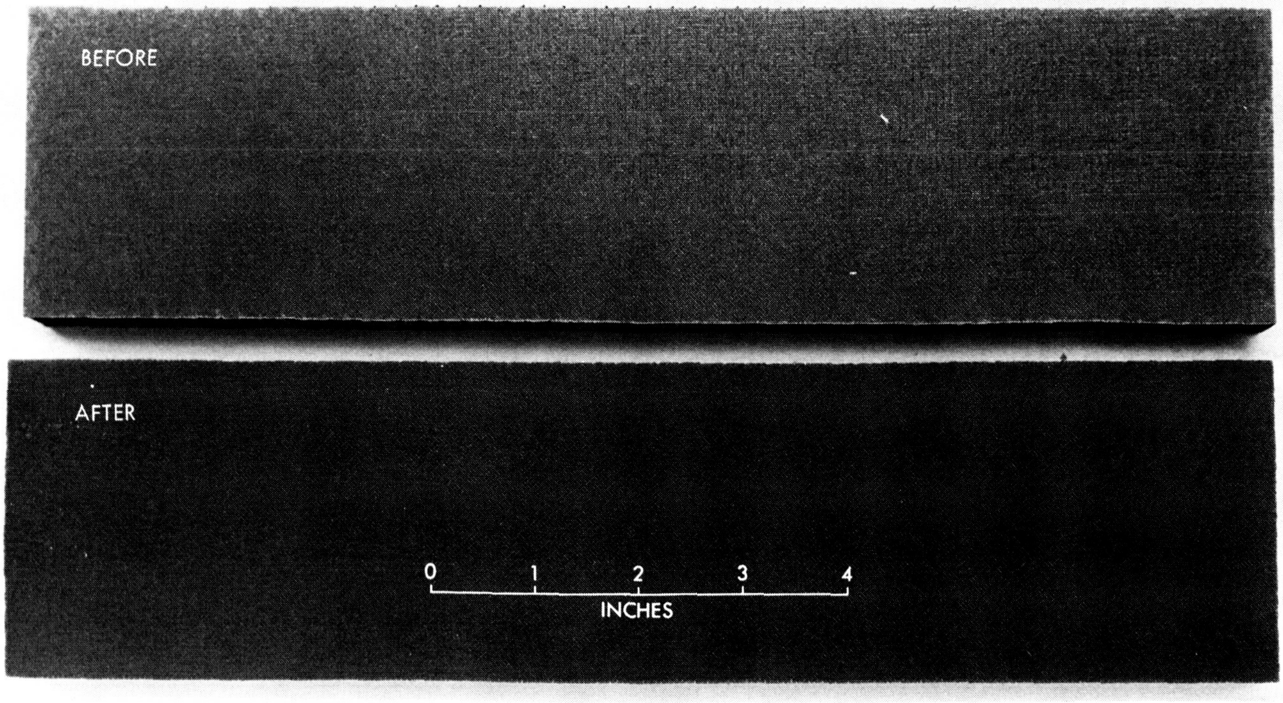

Fig. 59. Comparison of before and after sterilization samples

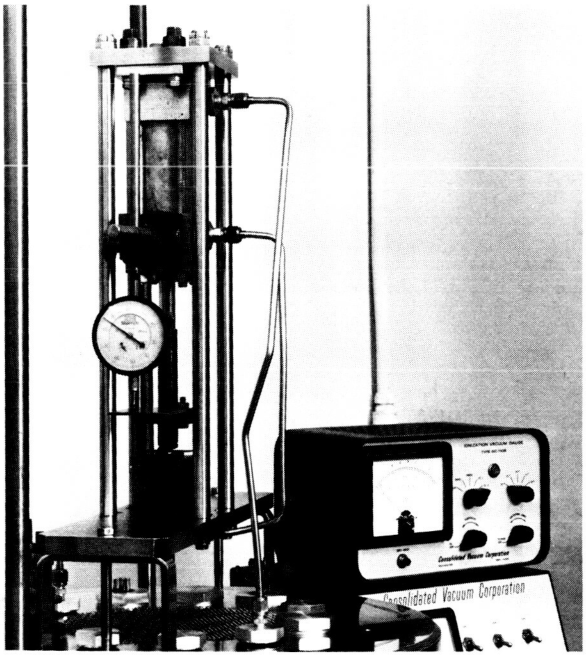

Fig. 60. Laminate flexure test setup in a vacuum

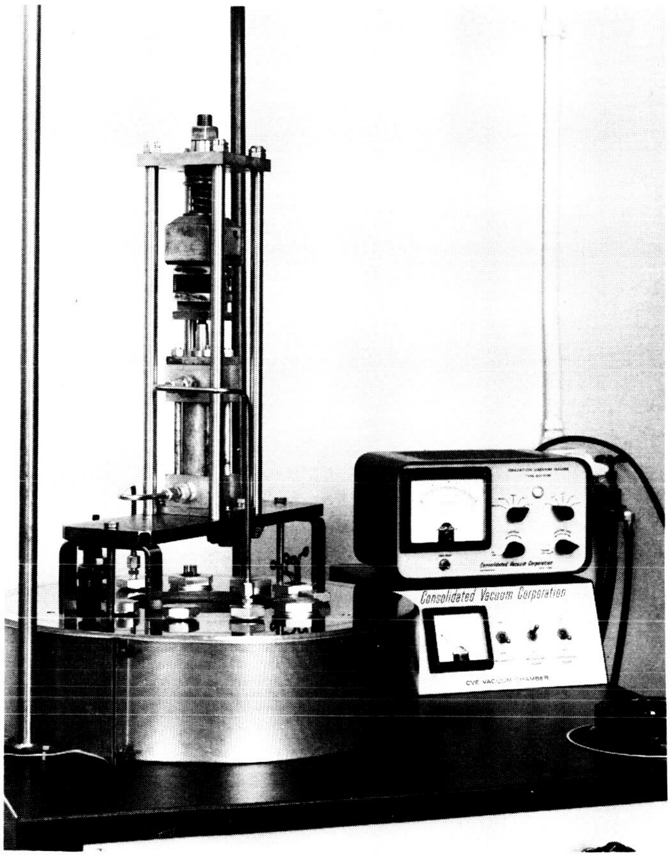

Fig. 61. Flatwise tension test setup in a vacuum

depending on whose data is used, it may be concluded that the mechanical properties of phenolic fiberglass composites do, or do not, degrade in a vacuum. An 18-in. bell jar system was converted to both a flexure test apparatus (ASTM D-790, Fig. 60) and a flatwise tension test apparatus (ASTM C-297, Fig. 61). The flatwise tension test data showed no change in strength in the vacuum, which means that tensile failure in the adhesive is not affected by pressure (gaseous species availability). The flexure tests also showed no change in strength in the vacuum, which indicated that — at least for this particular resin and configuration — the availability of gaseous species does not significantly affect toughness (resistance to crack propagation) or crazing.

C. Honeycomb-Sandwich Thermal Gradient Tests

To check the effects of assuming a 600°F maximum heat-shield/structure bond-line temperature on overall performance, it was necessary to develop a test that simulated short-time 600°F performance in the honeycomb sandwich. A standard, flatwise tension test was carried out on honeycomb-sandwich specimens where one face was held at room temperature and the other face was heated rapidly to 600°F by use of calrods in a copper support block (Fig. 62). Unfortunately, the best test conditions had about twice the dwell time at temperature and half the heat-up rate of the calculated case in mission studies. Results show that the 4-mil epoxy adhesive used in the present structure is probably borderline, but that a 7-mil epoxy-phenolic adhesive developed especially for the advanced development program performs quite adequately. Attempts are being made to have this unsupported epoxy-phenolic adhesive made in a thinner gage to make the weights more competitive.

D. Insert Retention Tests

A test apparatus was set up whereby the ability of the inserts to be pulled out of, or pushed into, the attachment ring could be evaluated. A photograph of a failed specimen in the test setup is shown in Fig. 63. When the inserts were pulled, the specimens failed at the major bend in the attachment ring, as shown in Fig. 63. A force of approximately 1200 lb was needed to fail the skin. For the 32 inserts, this is equivalent to trying to pull the payload from the aeroshell with a load of about 40,000 lb. Insert push tests showed crushing of the foam under loads of about 1800 lb, which is equivalent to a local pressure of about 7000 psi. A strength contribution due to the adhesive bond to the skin was obvious. Both values are more than enough to satisfy the design criteria.

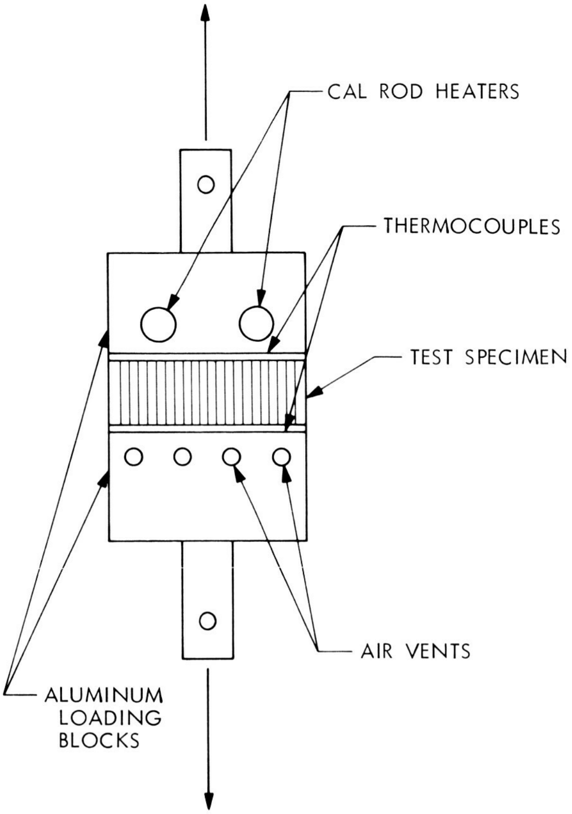

Fig. 62. Schematic of flatwise tension test with one hot face

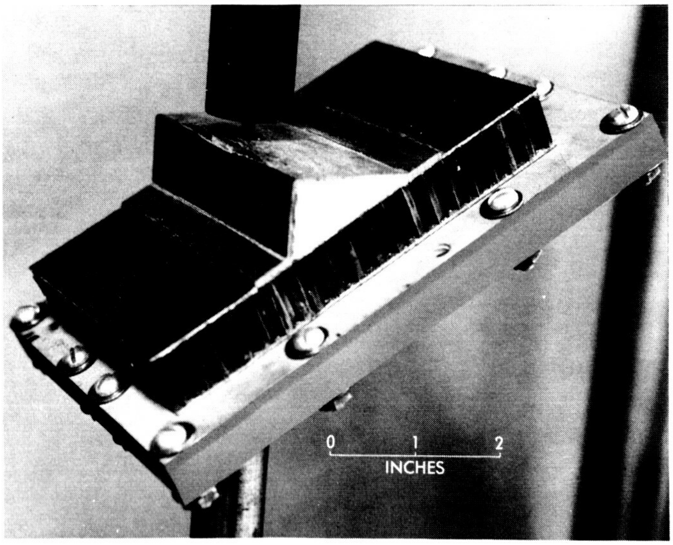

Fig. 63. Test setup for insert pull strengths

E. Core Splice Effects

The strength of standard core splices, both parallel and perpendicular to the core ribbon direction, had been evaluated in the advanced development program. These spliced specimens proved stronger; however, they were heavier. In the fabrication of the cone, though, the splice takes place along an approximately 22-deg angle which causes different distortions in the strain pattern during test. Additional specimens were made with overlap core splices along a 22-deg angle. When compared with the unspliced specimens tested at the same 22-deg angle, spliced specimens showed no change in flexure strength, either laterally or transverse to the splice. Failures in the spliced specimens were always directly adjacent to the shear zone, but both level and scatter were essentially equivalent.

F. Titanium Joining

Titanium lap shear and tensile tests were made to verify joint strength in both the adhesively bonded-doubler and welded configurations. Standard tensile tests on commercially pure titanium stock provide yield strengths of 55,000 psi. Typical welded specimens had joint efficiencies of 90%. Lap shear specimens duplicating the one-inch overlap in the structure showed strengths of 4000 psi and, generally, failed in the titanium rather than in the adhesive, since the overlap was excessive. Welded titanium rings were eventually used to save the few additional ounces typical in the doubler configurations.

G. Metal Dome—Ablator Joint

To allow free expansion at the joint between the metallic dome on the nose and the major structure with ablator, it was desirable to allow the ablator some local flexibility. Silicone elastomers have considerable flexibility, even in the filled form used in this fabrication. Calculations showed that the weakest portion of the joint design shown in Fig. 6 is the possibility of delamination along the heat-shield/structure interface, starting at the teflon gasket interface and propagating along the cone. A possible solution to this problem, which was not sufficiently developed to be incorporated into the actual fabrication, is the concept of using rows of small fiberglass loops circumferentially around the fore end of the cone. These loops would be buried in the ablator, providing a mechanical means of preventing ablator peel. An example of this loop form is shown in Fig. 64. Loops are sewn into one ply of preimpregnated cloth and then layed up on the other layers in the standard fashion. Some protection is needed during vacuum-bagging and cure to prevent crushing of the loops.

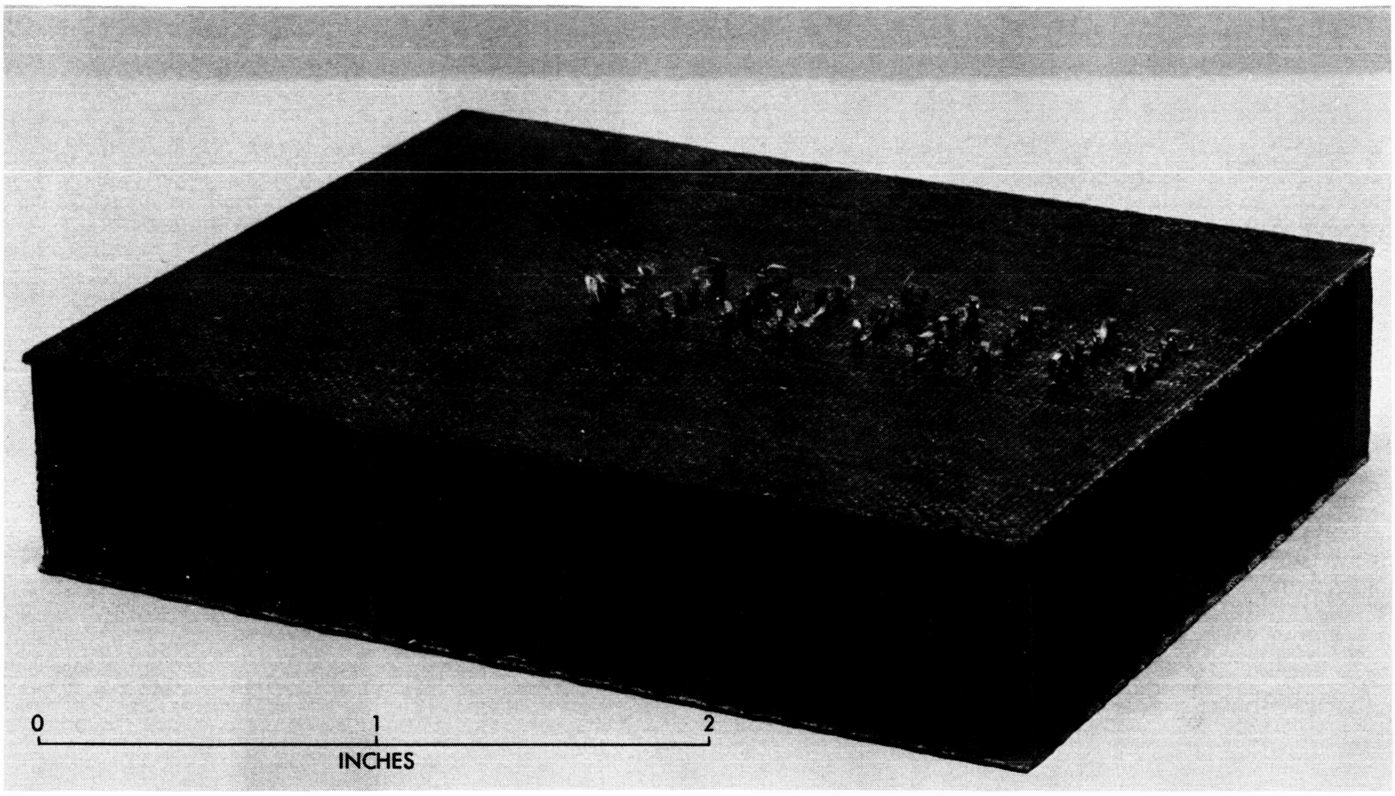

Fig. 64. Loop retainers for critical ablator joint

IX. Summary

A 6½-ft diameter aeroshell was designed for an early Mars atmospheric-entry-probe mission. This sphere-cone shape has (1) a spherical metallic nose for atmospheric composition measurements; (2) a 60-deg half-angle cone made from lightweight phenolic fiberglass honeycomb sandwich, (3) a short conical aft stiffening ring in the form of a titanium-phenolic fiberglass honeycomb-sandwich composite, and (4) a rollercoated elastomeric heat shield for ease of fabrication, light weight, and RF transparency.

The composite concept developed in an advanced development program was shown to have several advantages: (1) Phenolic fiberglass honeycomb-sandwich structures are lighter, easier to fabricate, and more reliable than minimum-gage aluminum-honeycomb sandwich structure. (2) Four plies of phenolic-impregnated 4-mil glass cloth applied at 45-deg rotations, with 4-mil epoxy film adhesive, and combined with a hexagonal-shaped phenolic fiberglass core that is formed in the partially cured state, give the lightest reproducible structure available with the current state of the art. (3) Elastomeric heat shields are major candidates for Mars missions, and roller-coated varieties provide most of the strength typical in molded samples.

The particular design for the mission under consideration requires 6 plies instead of 4 for the basic sandwich construction. Reinforced areas are required at three locations: (1) at the forward area of the cone at the joint between the metallic spherical nose and the structure, (2) at the half diameter of the aeroshell where the payload attaches to the structure, and (3) at the outer edge, where stiffening requirements have necessitated a supplementary conical ring. A complete description of the fabrication and inspection of the 6½-ft diameter aeroshell is given.

Appendix

Specification for Aeroshell Fabrication

I. Detail Part Fabrication

A. V-Ring and C-Ring

1. Seven plies E glass style 112 with Volan A finish and B-staged with Adlock 851 resin content 45, ±3%.
2. Lay up precut strips of prepreg with the warp of each ply aligned circumferentially, using ¼-in. overlap for splices.
3. Vacuum-bag and cure (standard cure ½ h at 300°F, 2 h at 350°F, unless otherwise noted).
4. Inspect (no wrinkles allowed).
5. Pot V-rings with M323V, except in local region near splice.

B. Attach Ring

1. Use two plies E glass style 112 next to tool followed by five plies E glass style 181 with Volan A finish and B-staged with Adlock 851 resin content 45, ±3%.
2. Lay up precut circular segments of prepreg (approximately 90 deg).
3. Vacuum-bag and cure (flow at 215°F and 50 psi, reduce to vacuum pressure, ½ h at 275°F, ½ h at 300°F, 2 h at 350°F).
4. Inspect (ensure proper tool release before proceeding).
5. Machine holes per JPL drawing.

C. Laminated Space Washers

1. Use 14 plies for inner washer and 10 plies for outer washer of E glass style 181 with Volan A finish and B-staged with Adlock 851 resin content 45, ±3%.
2. Lay up as square flat laminates with 45-deg rotation of plies.
3. Vacuum-bag and cure.
4. Machine to JPL drawing.

D. Insulators

1. Machine spacer and washer insulators from high-temperature phenolic stock to drawing configuration.

E. Titanium Skin

1. Cut out approximately 120-deg segments.
2. TIG seam-weld skins.
3. Check fit in tool after each weld.

F. Titanium U-Ring

1. Cut out approximately 120-deg segments.
2. Breakform into channel.
3. Stretchform into angle.
4. Anneal.
5. Reform.
6. Weld.
7. Inspect.
8. Grind.

G. Stainless Steel Nose Cap

1. Machine nose cap per drawing.

II. Aft Honeycomb Conical Subassembly

A. Titanium Outer Skin, U-Ring, and Honeycomb Core

1. Phosphate-fluoride clean titanium details.
2. Apply two layers of FM-96U (0.03 lb/ft^2) adhesive over entire titanium skin in tool.
3. Position U-ring and lock in place with supplemental pressure from a rubber gasket.
4. Cut and fit three precured honeycomb gore segments with ribbon in radial direction; splice, using a minimum 1-cell, maximum 2-cell overlap, and apply FM-40 foam adhesive between core and titanium U-ring.
5. Vacuum-bag and cure (1 h at 350°F).
6. Machine curvature on the core at outer edge per JPL drawing and machine inner surface flush with U-ring.
7. Apply a minimum amount of Epocast H1843 type 4, grade A, to outermost core cells to seal core edges.

B. Lay Up Inner Facesheet and V-Ring

1. Hand-clean titanium U-ring with Pasa-Jell 107.
2. Install potted V-ring with 1-in. doubler.
3. Apply M323V potting compound in V-ring region as required.
4. Apply FM-96U (0.03 lb/ft^2) adhesive over entire area.
5. Lay up four plies E glass style 112 with Volan A finish and B-staged with Adlock 851 resin content 45, ±3%.
6. Trim inner skin to match U-ring.
7. Vacuum-bag and cure.
8. Inspect (coin tapping).

III. Forward Conical Subassembly

A. Lay Up Outer Facesheet in Female Tool

1. Use six plies E glass style 112 with Volan A finish and B-staged with Adlock 851 resin content 45, ±3%.
2. Precut gore segments, overlapped ¼ in. circumferentially and a minimum of ¼ in. excess at forward and aft edge.
3. Rotate each succeeding ply 45 deg clockwise from previous ply.
4. Include 2 extra external plies at aft edge, 6 extra internal plies at fore edge, and 6 internal plies in a minimum 3-in.-wide doubler per drawing.
5. Place and center precured 0.12-in.-thick and 14.87-in. ID machined washer on flat section at fore end of core, and apply FM-96U adhesive to faying surface.
6. Use a metal ring pressure plate at forward section to eliminate voids at 30-deg transition.
7. Vacuum-bag and cure.
8. Reinforce aft edge of skin with copper tubing prior to removal from tool.

B. Lay Up Adhesive and Honeycomb Core to Outer Facesheet

1. Cut 8 honeycomb gore segments with ribbon in radial direction, preform using a minimum 1-cell, maximum 2-cell overlap splice, and vacuum-cure (2 h at 270°F).
2. Machine fore edge and prefit on outer facesheet.
3. Apply FM-96U (0.03 lb/ft^2) over entire area except at outer 2.5 in.
4. Apply additional layer of FM-96U (0.03 lb/ft^2) in two ½-in.-wide rings at upper and lower edge of 3-in. inside doubler to provide a satisfactory bond at region of core joggle.
5. Apply additional layer of FM-96U (0.03 lb/ft^2) in region of machined core surface at fore end of cone.
6. Apply M323V at forward edge of honeycomb.
7. Vacuum-bag, place pressure plate on forward ring to ensure flat surface and cure (1 h at 350°F).
8. Inspect (coin tap front bond).
9. Reset for machining, protecting aft edge, and clamping forward edge with disk tool.
10. Machine core at aft edge with attachment ring tool as extra holddown tool.
11. Machine rest of core and M323V at forward region.
12. Apply a minimum amount of Epocast H1843 type 4 grade A to outermost core cells to seal core edges.

C. Lay Up Inner Facesheet

1. Install potted V-ring with 1-in. doubler.
2. Apply M323V potting compound in V-ring region as required.
3. Apply FM-96U (0.03 lb/ft^2) over entire V-ring, core, and washer area.
4. Apply additional layer of FM-96U (0.03 lb/ft^2) in two ½-in.-wide rings at the upper and lower edge of the 3-in. ID doublers to provide a satisfactory bond at region of core joggle.
5. Apply additional layer of FM-96U (0.03 lb/ft^2) in region of machined core surface at forward end of cone.
6. Lay up 4 extra plies at fore edge, and 6 plies in a minimum 3-in.-wide doubler per drawing.
7. Lay up 6 plies of same E glass style 112 with Volan A finish and B-staged with Adlock 851 resin content 45, ±3%, rotating each ply 45-deg clockwise from previous ply.
8. Vacuum-bag and cure, using a forward assembly pressure tool as a fore pressure plate and the aft

ring with the aft bond tool to match markoffs on parts (vacuum-bag between tools).

9. Inspect (coin tapping).

IV. Final Assembly of Aeroshell

A. Adhesive Bonding Two Cones Together

1. Assemble parts and bond jigs together and check gap between mating surfaces.
2. Disassemble.
3. Apply FM-96 supported adhesive as required for measured gap.
4. Reassemble parts and jigs.
5. Apply M323V potting compound in *y* area and trowel to contour per drawing.
6. Install C-ring with 1-in. precured doublers cut back to tangency point.
7. Seal the two bond jigs at outer mating area, vacuum-bag, and cure (1 h at 350°F).

B. Attach Ring Installation

1. Place attach ring precured laminate in center bond tool.
2. Install inserts, using washers of adhesive common to faying surface.
3. Cure for 1 h at 350°F.
4. As a release aid, apply Teflon tape to outer surface of attachment ring, except on vertical surface, and replace ring in tool.
5. Apply M323V potting compound and trowel to flatness.
6. Apply FM-96 supported adhesive to faying surface on main cone.
7. Lower the center bond tool to mate with forward conical subassembly and forward bond jig.
8. Teflon tape edges of attachment ring to eliminate adhesive flash.
9. Apply necessary pressure to tool and cure (1 h at 350°F).
10. Release and inspect.

C. Installation of Stainless Steel Nose Cap

1. Install nose cap, insulators, and hardware.
2. Inspect alignment, ablator recess, and general configuration.

D. Contour Inspection

1. Install and center aeroshell assembly in sweep tool.
2. Sweep circumferentially at 7 positions.
3. Sweep radially at 16 positions.

References

1. Scholl, J. A., Dawson, J. B., and Koss, M., *Fabrication and Test of Lightweight Honeycomb Sandwich Structures, Final Report for JPL Contract No. 951612. Period August 1966 to October 1968.* Rohr Corporation.
2. Rung, Robert, Mason, Phillip, and Rosenbaum, Jacob, *Unsymmetrical Analysis of Shells of Revolution,* Report ADR 02-11-65.3. Grumman Aircraft Engineering Corp., Bethpage, L.I., N.Y., Dec. 1965.
3. *Environmental Specification, Voyager Capsule Flight Experiment, Type Approval and Flight Acceptance Test Procedures for the Heat Sterilization and Ethylene Oxide Decontamination Environments,* JPL Sterilization Specification VOL-50503-ETS. Jet Propulsion Laboratory, Pasadena, Calif., Jan. 12, 1966.
4. Boundy, R. A., "Nonmetallic Materials for Unmanned Spacecraft," *The Effects of the Space Environment on Materials, Proceedings of the 11th National Symposium and Exhibit, April 19–21, 1967, St. Louis, Mo.,* pp. 193–204. Society of Aerospace Material and Process Engineers, 1967.
5. *Polymers for Spacecraft Application, Final Report for JPL Contract No. 950745,* Stanford Research Institute, Menlo Park, Calif., Sept. 15, 1967.